BRL

AD

REPORT NO. 1475

THE GAS FLOW IN GAS-OPERATED WEAPONS

by

Joseph H. Spurk

February 1970

U.S. ARMY ABERDEEN RESEARCH AND DEVELOPMENT CENTER
BALLISTIC RESEARCH LABORATORIES
ABERDEEN PROVING GROUND, MARYLAND

60

B A L L I S T I C R E S E A R C H L A B O R A T O R I E S

REPORT NO. 1475

February 1970

THE GAS FLOW IN GAS-OPERATED WEAPONS

Joseph H. Spurk

Exterior Ballistics Laboratory

RDT&E Project No. 1T061102A33D

A B E R D E E N P R O V I N G G R O U N D, M A R Y L A N D

B A L L I S T I C R E S E A R C H L A B O R A T O R I E S

REPORT NO. 1475

JHSpurk/so
Aberdeen Proving Ground, Md.
February 1970

THE GAS FLOW IN GAS-OPERATED WEAPONS

ABSTRACT

In gas-operated weapons, the time-varying pressure in the barrel is fed through a duct into a cylinder. The piston in the cylinder is displaced by the pressure and operates on a mechanism which extracts the spent cartridge and completes the next loading cycle.

The theory presented here predicts the pressure history in the cylinder and the motion of the piston for a given pressure and temperature history in the barrel.

TABLE OF CONTENTS

		Page
	ABSTRACT	3
	LIST OF ILLUSTRATIONS	7
	LIST OF SYMBOLS	9
I.	INTRODUCTION	15
II.	METHOD OF APPROACH	16
III.	ANALYSIS	21
	A. The Flow in the Cavity	21
	B. The Flow in the Duct	23
	C. The Outer Problem	27
	D. The Inner Problem	39
	E. The Composite Solution for the Flow in the Duct	44
IV.	COMPARISON WITH EXPERIMENT	48
V.	CONCLUSION	53
	ACKNOWLEDGEMENT	55
	ADDENDUM -- TREATMENT OF PORT AS AREA DISCONTINUITY	56
	REFERENCES	60
	APPENDIX A -- DERIVATION OF EQUATION (36)	61
	APPENDIX B -- DERIVATION OF APPROXIMATE FLOW RELATIONS	62
	DISTRIBUTION LIST	65

LIST OF ILLUSTRATIONS

Figure		Page
1.	Design Sketch of M-16 Rifle	17
2.	Idealized Geometry for M-16 Rifle	20
3.	Outer Solution Variation of Mach Number in Gas Tube	32
4.	Sketch for Derivation of Approximate Flow Relations	38
5.	X,T Diagram for Inner Solution--Nozzle at Port	42
6.	Comparison of Experimental and Theoretical Bolt Carrier Pressures for M-16 Rifle (Round 52)--Nozzle at Port . . .	52
7.	Comparison of Experimental and Theoretical Bolt Carrier Pressures for M-16 Rifle (Round 52)--Area Discontinuity at Port	54
8.	Sketch for Compressible Flow Treatment of Area Discontinuity at Port	57
9.	X,T Diagram for Inner Solution--Area Discontinuity at Port.	59

LIST OF SYMBOLS

NOTE: 1. Dimensional quantities are indicated by bars; non-dimensionalizing factors are given in Equations (16).

2. Functions p, ρ, h, and u first denote solution to Equations (17), (18), and (19); then denote solution to Equations (21) with the subscript "1" dropped (outer solution).

$\bar{A}_c$, $\bar{A}_e$, $\bar{A}_v$ — cross-sectional areas of cavity, cavity entrance, and vent, respectively [m^2]

$\bar{A}_{min}$, $\bar{A}_p$ — areas at throat and exit of port, respectively [m^2]

$\bar{D}$ $(=[4\bar{A}_e/\pi]^{1/2})$ — cross-sectional diameter of gas tube [m]

$\bar{F}$ — friction force in gas tube flow (Eq. (10)) [N /kg]

$\bar{H}$ — $(=\bar{h})$ enthalpy per unit mass in inner problem [Nm/kg]

$\bar{J}$ — $\equiv (1/2)\, f\, \bar{c}_p\, \bar{\rho}\, \bar{u}$ [Nm/(m^2 sec deg K)]

K_1 — $= 0$ for $\bar{x}_B < \bar{x}_{Bv} - \bar{r}_v$

$= [\frac{2}{\gamma+1}]^{(\gamma+1)/[2(\gamma-1)]}$ for $\bar{x}_B > \bar{x}_{Bv} - \bar{r}_v$

K_2 — $= 0$ for $\bar{x}_B < \bar{x}_{Bv} - \bar{r}_v$

$= [\frac{2}{\gamma+1}]^{(3\gamma-1)/[2(\gamma-1)]}$ for $\bar{x}_B > \bar{x}_{Bv} - \bar{r}_v$

K_F, K_B — resistance coefficients due to friction and bends, respectively (Eq. (39)).

M — Mach number $(= \bar{u}/\bar{a})$

M_s — $\equiv \bar{U}_s/\bar{A}_1$

$\bar{M}_B$ — mass of bolt carrier [kg]

LIST OF SYMBOLS (CONT'D)

$\bar{P}$ ($= \bar{p}$) pressure in inner problem [N /m^2]

Re Reynolds number (based on cross-sectional diameter of gas tube)

$2\bar{R}$ $\equiv \bar{U}_3, + [2/(\gamma-1)]\, \bar{A}_3,$ -- Riemann invariant [m/sec]

$\bar{R}_{gas}$ effective gas constant for powder gas [Nm/(kg deg K)]

$\bar{T}$ $\equiv \bar{t}/\delta(\epsilon)$--time variable for inner problem [sec]

$\bar{U}$ ($= \bar{u}$) gas velocity in inner problem [m/sec]

$\bar{U}_s$ velocity of initial shock wave in gas tube (inner problem)[m/sec]

$\bar{V}_c$ volume of cavity [m^3]

$\bar{V}_{ci}$ $= \bar{V}_c$ ($\bar{t} = 0$)

$\bar{X}$ ($= \bar{x}$) distance variable for inner problem [m]

$\bar{a}$ speed of sound [m/sec] ($= \{\gamma \bar{p}/\bar{\rho}\}^{1/2}$)

$\bar{c}_p$ specific heat at constant pressure [Nm/(kg deg K)]

$\bar{c}_v$ specific heat at constant volume [Nm/(kg deg K)]

$\bar{e}$ ($\equiv \bar{c}_v\, \bar{\theta}$) internal energy per unit mass [Nm/kg]

f friction factor ($= \bar{F}\, \bar{D}/\{2\bar{u}^2\}$). (Eqs. (13) and (39))

g gain factor (Equation (46))

$\bar{h}$ enthalpy per unit mass [Nm/kg]

$\bar{k}$ thermal conductivity of powder gas [(kg m)/(sec^3 ^oK)]

$\bar{\ell}$ length of gas tube [m]

$\bar{m}$ $\equiv \bar{A}_e\, \bar{\rho}_e\, \bar{u}_e$ [kg/sec]

$\bar{p}$ pressure [N/m^2]

p_{crit} $\equiv p_g\, [2/(\gamma+1)]^{\gamma/(\gamma-1)}$

$\bar{q}$ heat transferred in duct flow [Nm/(kg sec)] (Eq. (14))

$\bar{r}_v$ radius of vent cross-section [m]

$\bar{t}$ time [sec]

$\bar{u}$ gas velocity [m/sec]

$\bar{v}_B$ velocity of bolt carrier with respect to bolt [m/sec]

$\bar{x}$ distance from port in gas tube [m]. (coordinate in Equations (17), (18), and (19)

$\bar{x}_B$ displacement of bolt carrier [m]

$\bar{x}_{BE}$ maximum displacement of bolt carrier [m]

$\bar{x}_{Bv}$ location of center of vent [m]

α_e contraction coefficient--backward flow from cavity into duct

α_p contraction coefficient--backward flow from duct into port

α_g contraction coefficient--forward flow from gun barrel into port

β $\equiv U(X,T)_{visc}/U(X,T)_{invisc}$

$\tilde{\beta}$ average value of β in interval $0 < \bar{t} < \bar{\ell}/\bar{U}_{2\ visc}$

γ effective ratio of specific heats of gas

$\tilde{\gamma}$ exponent in p_g, θ_g relation (Eq. (57))

$\hat{\gamma}$ ratio of specific heats for gas initially present in gas tube ($\simeq 1.4$ for air)

$\delta(\epsilon)$ gage function for inner problem time variable

ϵ $\equiv \bar{\ell}/[\bar{\tau}\ \tilde{a}_g(0)$ --asymptotic expansion parameter

$\bar{\epsilon}/\bar{D}$ relative roughness of duct (Table 3)

$\bar{\theta}$ temperature [deg K]

$\bar{\theta}_{tot}$ total temperature in gas tube [deg K]

$\bar{\Lambda}$ ($= \bar{a}$) velocity of sound in inner problem [m/sec]

LIST OF SYMBOLS (CONT'D)

$\bar{\mu}$ viscosity coefficient of powder gas [kg/(m sec)]

$\bar{\rho}$ density [kg/m^3]

$\bar{\Sigma}$ entropy per unit mass [N m/(kg deg K)]

$\bar{\tau}$ characteristic time of pressure variation at port [sec]

$\bar{\tau}_w$ wall shearing stress in gas tube [N/m^2] ($= \frac{1}{2} f \bar{\rho} \bar{u}^2$)

$\bar{\Phi}$ forces on bolt carrier [N]

$\bar{\Omega}$ ($= \bar{\rho}$) density in inner problem [kg/m^3]

ω $\equiv \bar{A}_p/\bar{A}_{min}$

Subscripts

c bolt chamber

comp,e composite solution at entrance to cavity

e entrance to cavity

g gun barrel at port station (stagnation conditions)

i initial value ($\bar{t} \leq 0$)

p port exit (entrance to gas tube)

s shock wave

tot total

v vent

w wall of gas tube

1,2 first and second approximation to flow variables in gas tube, Equation (20)

1,2,3,3′ regions of flow in X,T diagram (Figure 5)

1,II supersonic and subsonic values of flow variables at shock wave (when present) in gas tube

Superscripts

*	port throat
-	dimensional quantity

I. INTRODUCTION

In gas operated weapons or in control systems a high pressure, high temperature supply of gas is used to operate certain mechanisms. The crucial problem presents itself in the following form: At a given point, A, in the system, pressure and temperature are prescribed as a function of time due to the inherent operation characteristics of the system. This pressure is communicated through a duct to another point, B, in the system where the gas is used to operate a mechanism; for example, extract a spent cartridge and impart enough momentum to the bolt so that the next round may be positioned in the chamber. It is desired to predict the pressure and other variables at point B as a function of time. The magnitude and time history of this pressure can be crucial to the whole operation cycle. In the example cited above, the pressure pulse must not cause extraction at too early a stage, when the cartridge is still pressed to the wall of the chamber by the pressure in the chamber; on the other hand the pressure history must be such that sufficient momentum is transferred to the bolt to operate the weapon. The pressure history is coupled to the rate at which work is extracted at B from the gas and also to the nature of the flow of gas between A and B. In this report an analysis is developed which describes the time history of pressure and temperature at point B for prescribed condition at A in the practically important case where the characteristic time of the pressure pulse at B is large compared to the time an acoustic signal needs to travel from A to B.

The analysis is developed on the specific example of the M-16 rifle where time varying pressure is fed from a port in the barrel (point A) to the bolt cavity (point B) where the pressure is used to unlock the bolt, extract the cartridge and supply sufficient momentum to the bolt carrier so that the next loading cycle can be completed. The analysis applies, however, equally well to other gas operated weapons and should find application in rocket control systems where high pressure gas is used to operate jet or surface controls.

II. METHOD OF APPROACH

For purposes of orientation, Figure 1 may be consulted. This shows a design drawing of the gas system of the M-16 rifle. As mentioned before, hot, high pressure powder gases are extracted from the barrel and fed into the bolt chamber by a duct. The pressure variation with time at the port is determined by the gas flow in the barrel. The mass flow through the port is small compared to the mass flow in the barrel itself, and the effect of mass removal is negligible on the pressure history at the port. Thus, the pressure and temperature may be considered prescribed and known, say from an interior ballistics analysis of the weapon. The hot gases expand in the bolt cavity, thereby accelerating the bolt carrier, C. Unlocking of the bolt, D, is accomplished after the carrier has traveled a certain distance, at which distance vent holes are laid free and the gas in the bolt carrier expands to atmosphere. At this distance the bolt carrier engages the bolt and cartridge, and extraction is accomplished by transferral of energy and momentum of the carrier to the bolt and cartridge. The residual momentum and energy of the bolt carrier is sufficient to complete the cycle of cocking the weapon and positioning a new cartridge in the chamber. It is the object here to predict for a given pressure and temperature at the port the motion of the bolt carrier referenced in time to the rise of pressure at the port. The motion of the bolt carrier is governed by the pressure and temperature in the bolt carrier cavity.

It is natural to divide the analysis into two parts. The first is the determination of the "space averaged" pressure and temperature in the bolt carrier cavity for given flow conditions at the entrance of the cavity. In general, these depend on the conditions in the cavity. It will be shown in Section III.A that conservation of energy and mass together with the equation of motion of the carrier, which here takes the place of conservation of momentum, uniquely determine the conditions in the cavity and the motion of the carrier. The second part considers the flow from the port to cavity. The unsteady flow in the pipe is quite complex and is indeed not even amenable to numerical computations without

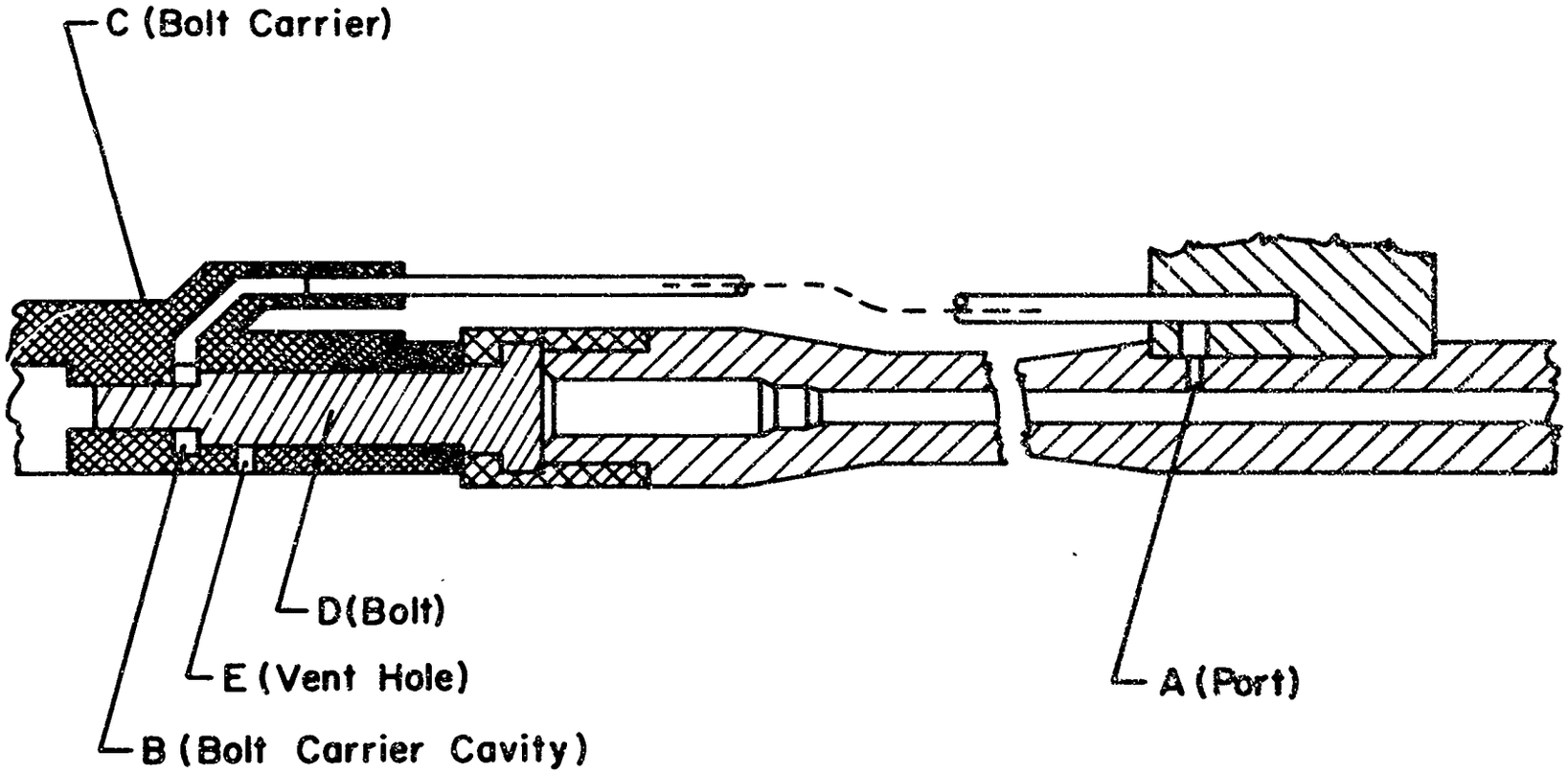

Figure 1. Design Sketch of M-16 Rifle

considerable simplifications. Such a simplification is offered by considering the flow to be one-dimensional; i.e., flow variables are assumed constant over the cross section of the duct, so that the flow variables depend only on $\bar{x}$, the distance along the axis, and on time. Implicitly, this assumes that conversion of frictional work to heat and conduction of heat occur instantaneously and uniformly over the entire cross section.

It is usual to introduce friction (and heat transfer) even in time dependent compressible flow according to the practice in hydraulics by means of a friction coefficient f defined by $\bar{F} = 2 f \bar{u}^2/\bar{D}$ where $\bar{F}$ is the friction force per unit mass. The friction coefficient f, however, is not known in unsteady turbulent flow and its prediction would indeed require the solution of the full problem since the coefficient of friction will depend on the entire flow history. Customarily, the friction coefficient for steady flow is, therefore, used and the few experiments done indicate this to be a good approximation[1] as long as no separation occurs. However, it is well to keep in mind that this assumption is satisfactory only for nearly steady flow.

It will be shown in Section III.C that the flow here can be reduced to a quasisteady flow except for the very early phases when the flow is being established. For the quasisteady regime, the frictional effects may be justifiably included by using the steady friction coefficient. For this phase of the flow, pressure and momentum losses due to sudden enlargements or constrictions are included in the analysis within the framework of one-dimensional quasisteady flow. Losses due to the various bends in the duct can, for large $\bar{\ell}/\bar{D}$ of the duct, be included by loss coefficients. These losses will be treated as a distributed resistance and accounted for in an overall friction coefficient.

For the very early stages, the flow is truly unsteady and it is not possible to include the frictional effects using a steady friction coefficient, nor is it possible to consider the bends in the tube as distributed resistances. This early stage involves a strong shock, which actually starts the flow; this shock will be reflected and diffracted and also influenced by friction and heat transfer in a complex

way not accessible to analysis at this time. The first stage will, therefore, be treated entirely without friction and discarding all possible reflections, the only justification being that this first stage is of very short duration compared to the total flow time. As will be shown in Section III.D , the first stage essentially introduces a delay time between the pressure rise at the port and the pressure rise in the cavity. The net effect of neglecting friction and shock reflections in the first stage will be to predict a delay time somewhat too small. However, this delay time has been observed experimentally in numerous tests[2] and a correction to the theoretical value is possible, thus accounting for the observable effect of friction and shock reflections in the first stage. The gas will be considered a calorically and thermally perfect gas; thus, the ratio of specific heats and the gas constant will be considered constant and given, say from the interior ballistic analysis of the weapon. Because of the high pressure and density the assumption of equilibrium for the gas phase of the propellant can be safely made; however, there is nonequilibrium between the solid and the gas phase of the propellant in the barrel itself and also in the duct. Within certain temperature and density ranges it is always possible to approximate the real gas behavior by an ideal gas behavior as long as the gas phase is in thermodynamic equilibrium. This approximation is commonly made in the standard interior ballistic treatment, and performance predictions based on this assumption are apparently in good agreement with experiment. Therefore, assumption of equilibrium and indeed perfect gas behavior is expected to be adequate also, since the primary purpose here is to clear up the fluid dynamic aspects. Correction factors accounting for real gas effects may be applied to the results found on the basis of perfect gas behavior as shown, for example, in reference 3. It should be mentioned that a rigorous nonequilibrium treatment of the gas flow is not possible because the kinetics of powder gas reactions are not sufficiently understood.

According to the assumption made above, the analysis will be based on the simplified geometry shown in Figure 2. The area restriction at

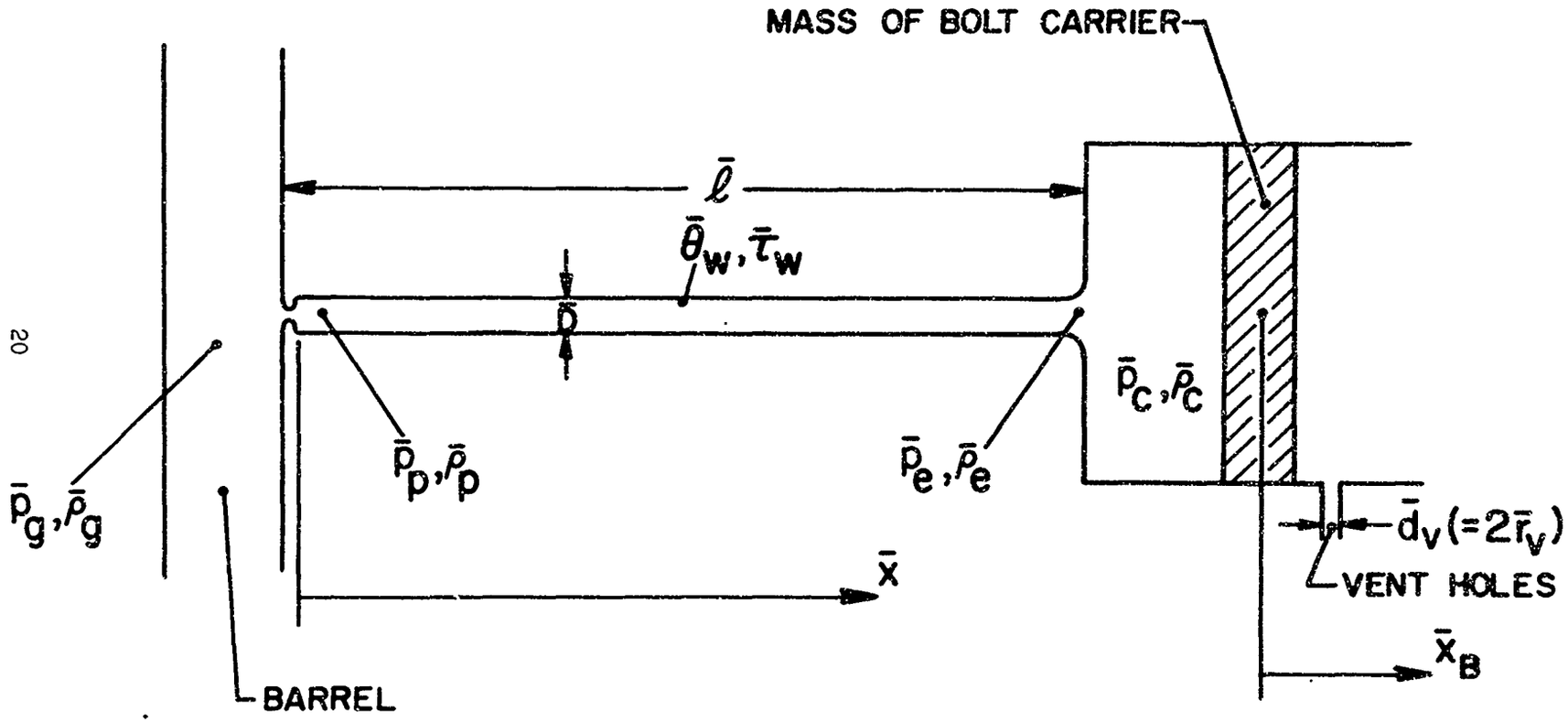

Figure 2. Idealized Geometry for M-16 Rifle

the port will be treated as a supersonic nozzle of zero length when the flow into the duct is supersonic, as is indicated on Figure 2.* The duct is considered a straight tube of constant inner cross section, with all losses resulting from bends and sudden area changes taken into account as discussed above.

Heat transfer from the gas to the wall is assumed to leave the wall temperature unchanged; this assumption allows uncoupling of the fluid dynamic problem from the heat conduction problem in the duct, and is a good one for the small Fourier-numbers of interest here.

III. ANALYSIS

A. The Flow in the Cavity

The average properties in the cavity are determined by the conservation equations of mass and energy and by the equation of motion of the bolt carrier.

Let
$$\bar{m} = \bar{A}_e \, \bar{\rho}_e \, \bar{u}_e \tag{1}$$

be the mass flow into the cavity, where $\bar{A}$ is an area**, $\bar{\rho}$ the gas density and the $\bar{u}$ the gas velocity, and where the subscript designates the location of these quantities in accordance with Figure 2. Conservation of mass gives

$$\bar{m} = (\bar{V}_{ci} + \bar{A}_c \, \bar{x}_B) \, \frac{d\bar{\rho}_c}{d\bar{t}} + \bar{A}_c \, \bar{\rho}_c \, \bar{v}_B + K_1 \, \bar{A}_v \, (\gamma \, \bar{p}_c \, \bar{\rho}_c)^{\frac{1}{2}} \tag{2}$$

The first term on the right side is due to the change of density in time in the cavity; the second term is due to the change in cavity size; and the third term is the term due to venting.

Accordingly, $K_1 = 0$ for $\bar{x}_B < \bar{x}_{Bv} - \bar{r}_v$, and $K_1 = [2/(\gamma+1)]^{(\gamma+1)/2(\gamma-1)}$ for $\bar{x} > \bar{x}_{Bv} - \bar{r}_v$, where $\bar{x}_{Bv}$ and $\bar{r}_v$ are the center location and radius, respectively, of the circular vent.

*The case where the port is treated as an area discontinuity is discussed in the Addendum.

**Dimensional quantities are indicated by bar.

Here, it has been assumed that p_c is always much larger than the ambient pressure, so that venting occurs with sonic velocity. Mass losses due to leakage may be included in this equation by an obvious extension.

Heat transfer to the wall of the cavity may be neglected, since the average gas velocity in the cavity is small so that convection is negligible.

Conservation of energy may then be written as

$$\bar{m}\,\bar{h}_{e\,tot} = \frac{d}{d\bar{t}}\left[\bar{\rho}_c\,\bar{e}_c\,\bar{V}_c + \frac{1}{2}\,\bar{\rho}_c\,\bar{v}_B^{\,2}\,\bar{V}_c + \bar{A}_c\int_0^{\bar{t}}\bar{p}_c\,\bar{v}_B\,d\bar{t}\right] +$$

$$K_1\,\bar{e}_c\,\bar{A}_v\,(\gamma\bar{\rho}_c\bar{p}_c)^{1/2} + K_2\,\bar{A}_v\bar{p}_c\,(\gamma\,\bar{p}_c/\bar{\rho}_c)^{1/2} + \qquad (3)$$

$$K_2\bar{A}_v\gamma\bar{p}_c\,(\gamma\bar{p}_c/\bar{\rho}_c)^{1/2}$$

The terms in the square bracket are the thermal energy of the gas in the cavity, the kinetic energy of gas in the cavity and the work done by the gas in the cavity. The three other terms are the energy losses due to venting. For the constant K_2 we have

$$K_2 = 0 \quad \text{for } \bar{x}_B < \bar{x}_{Bv} - \bar{r}_v; \quad K_2 = [2/(\gamma+1)]^{(3\gamma-1)/2(\gamma-1)} \quad \text{for } \bar{x}_B > \bar{x}_{Bv} - \bar{r}_v$$

For the circular vent

$$\bar{A}_v = (\bar{x}_B - \bar{x}_{Bv})\,[\bar{r}_v^{\,2} - (\bar{x}_B - \bar{x}_{Bv})^2]^{1/2} + \bar{r}_v^{\,2}\,[\tfrac{\pi}{2} + \sin^{-1}[(\bar{x}_B - \bar{x}_{Bv})/\bar{r}_v]]$$

$$\text{for} \qquad \bar{x}_{Bv} - \bar{r}_v \le \bar{x}_B \le \bar{x}_{Bv} + \bar{r}_v$$

$$\bar{A}_v = \pi\,\bar{r}_v^{\,2} \qquad \text{for} \qquad \bar{x}_{Bv} + \bar{r}_v \le \bar{x}_B$$

The volume $\bar{V}$ of the cavity is given by:

$$\bar{V}_c = \bar{V}_{ci} + \bar{A}_c\,\bar{x}_B$$

The term $\bar{m}\,\bar{h}_{e\ tot}$ is, of course, the flux of enthalpy into the cavity, where

$$\bar{h}_{e\ tot} \equiv \bar{p}_e/\bar{\rho}_e + \bar{e}_e + \bar{u}_e^{\,2}/2 \quad .$$

The equation of motion for the bolt carrier is given by:

$$\frac{d\,\bar{v}_B}{d\bar{t}} = \bar{p}_c\,\bar{A}_c\,\bar{M}_B^{\,-1} + \Phi\,\bar{M}_B^{\,-1} \tag{4}$$

$$d\bar{x}_B/d\bar{t} = \bar{v}_B$$

Φ signifies external forces on the bolt carrier, such as friction on the bolt. At the end of the bolt carrier travel $\bar{v}_B$ and $d\bar{v}_B/d\bar{t}$ are set equal to zero.

The conservation equations and the equation of motion of the bolt are three equations for the five unknowns, $\bar{x}_B$, $\bar{p}_c$, $\bar{\rho}_c$, $\bar{\theta}_c$ and $\bar{e}_c$.

The problem is rendered complete by the addition of a thermal and a caloric equation of state, thus:

$$\bar{e} = \bar{c}_v\bar{\theta} \qquad \text{and} \qquad \bar{p} = \bar{R}_{gas}\,\bar{\rho}\,\bar{\theta} \tag{5}$$

B. <u>The Flow in the Duct</u>

The flow in the duct is a mixed initial and boundary value problem. Using the usual notation for pressure, velocity and sound velocity, $\bar{p}$, $\bar{u}$, $\bar{a}$, respectively, the initial conditions are

$$\bar{t} = 0;\ \bar{x} > 0 : \bar{p}\,(\bar{x},0) = \bar{p}_i\ ; \quad \bar{a}\,(\bar{x},0) = \bar{a}_i\ ;\ \bar{u}\,(\bar{x},0) = 0 \tag{6}$$

$$\bar{x} < 0 : \bar{p}\,(\bar{x},0) = \bar{p}_g\,(0);\ \bar{a}\,(\bar{x},0) = \bar{a}_g\,(0);\ \bar{u}\,(\bar{x},0) = 0$$

For $\bar{u}_p > \bar{a}_p$ the boundary $\bar{x} = 0$ is spacelike and three input data at $\bar{x} = 0$ determine the solution for nonisentropic flow. Thus,

$$\bar{t} > 0,\ \bar{x} = 0 : \bar{p}\,(0,\bar{t}) = \bar{p}_p\,(\bar{t});\ \bar{a}\,(0,\bar{t}) = \bar{a}_p(\bar{t})\ ;\ u\,(\bar{0},\bar{t}) = \bar{u}_p\,(\bar{t}) \tag{7}$$

For $\bar{u}_p < \bar{a}_p$ the line $\bar{x} = 0$ is timelike corresponding to the fact that only two characteristics enter the region of interest. Thus, two data along $\bar{x} = 0$ are required:

$$\bar{t} > 0,\ \bar{x} = 0:\ \bar{p}(0,\bar{t}) = \bar{p}_p(t),\ \bar{u}(0,\bar{t}) = \bar{u}_p(\bar{t}) \tag{8}$$

By virtue of the fact that the nozzle length is very small, the conditions at the exit of the nozzle (subscript p) follow the conditions in the barrel (subscript g) instantaneously.

At $\bar{x} = \bar{\ell}$ no boundary condition can be prescribed for $\bar{u}_e > \bar{a}_e$ corresponding to the fact that no characteristic reaches the space $\bar{x} < \bar{\ell}$ for $d\bar{t} > 0$. For $\bar{u}_e < \bar{a}_e$ the characteristic given by $d\bar{x}/d\bar{t} = \bar{u} - \bar{a}$ reaches into the region $\bar{x} < \bar{\ell}$ and one condition at $\bar{x} = \bar{\ell}$ must be prescribed. Thus,

$$\bar{t} > 0,\ \bar{x} = \bar{\ell}:\ \bar{p}(\bar{\ell},\bar{t}) = \bar{p}_c(\bar{t}) \tag{8a}$$

Subject to the above initial and boundary values the following set of equations describes the one-dimensional flow in the duct.

Continuity:

$$\frac{\partial \bar{\rho}}{\partial \bar{t}} + \frac{\partial\,(\bar{\rho}\,\bar{u})}{\partial \bar{x}} = 0 \tag{9}$$

Momentum:

$$\frac{D\,\bar{u}}{D\,\bar{t}} + \frac{1}{\bar{\rho}}\frac{\partial\,\bar{p}}{\partial\,\bar{x}} + \bar{F} = 0 \tag{10}$$

Energy:

$$\frac{1}{\bar{\rho}}\frac{\partial \bar{p}}{\partial \bar{t}} + \bar{q} = \frac{D}{D\bar{t}}\left(\frac{\bar{u}^2}{2} + \bar{h}\right), \text{ or} \tag{11}$$

$$\bar{u}\,\bar{F} + \bar{q} = \frac{D\bar{e}}{D\bar{t}} - \frac{\bar{p}}{\bar{\rho}^2}\frac{D\bar{\rho}}{D\bar{t}} \tag{11a}$$

Instead of the energy equation the entropy equation may be used:

$$\bar{\theta}\,\frac{D\bar{\Sigma}}{D\bar{t}} = \bar{u}\,\bar{F} + \bar{q} \tag{12}$$

Here, $D/D\bar{t} \equiv \partial/\partial\bar{t} + \bar{u}\,\partial/\partial\bar{x}$ is the material derivative.

These equations are complemented by the equation of state (5). The hydrodynamic friction force $\bar{F}$ is introduced as

$$\bar{F} = \frac{\bar{D}\,\pi\,\bar{\tau}_w\,d\bar{x}}{\bar{\rho}\,\pi\,(\bar{D}^2/4)\,d\bar{x}} = \frac{4\,\bar{\tau}_w}{\bar{\rho}\,\bar{D}} = \frac{2\,f\bar{u}^2}{\bar{D}} \tag{13}$$

with $\bar{\tau}_w = \frac{1}{2}\,f\,\bar{\rho}\,\bar{u}^2$, the wall shearing stress.

The amount of heat transferred per unit time per unit mass is:

$$\bar{q} = -\frac{\bar{J}\,(\bar{\theta}_g - \bar{\theta}_w)\,\bar{D}\,\pi\,d\bar{x}}{(\bar{D}^2/4)\,\pi\,\bar{\rho}\,d\bar{x}} = \frac{-4\bar{J}\,(\bar{\theta}_g - \bar{\theta}_w)}{\bar{\rho}\,\bar{D}} \tag{14}$$

Reynolds analogy for turbulent flow gives:

$$\bar{J} = \frac{f\,\bar{c}_p\,\bar{\rho}\,\bar{u}}{2} \tag{15}$$

This relation is not strictly fulfilled for turbulent flow in a pipe because of the effect of the laminar sublayer. Here, it is assumed that this relation holds strictly; this amounts to setting the recovery factor equal to unity.

The above system of equations is hyperbolic and has the characteristic directions

$$d\bar{x}/d\bar{t} = \bar{u} \pm \bar{a} \quad \text{and} \quad d\bar{x}/d\bar{t} = \bar{u} \ ,$$

the latter being the differential equation for the particle path and the former the differential equations for the other two characteristic directions. The compatibility conditions may be found by standard techniques and are given in many textbooks, see for example reference 4. Thus the flow in the duct may be computed by the method of characteristics. However, such a computation for the present case is very time-consuming at best. Since the acoustic transit time $\bar{\ell}/\bar{a}$ is very short compared to the total duration $\bar{\tau}$ of the flow, the computation has to be extended to large times and this will lead to an appreciable error unless the grid size is very small. It should be pointed out that characteristic computation for nonisentropic flow is considerably more complex

since the particle path has to be computed together with the two other characteristics. A further complication arises from the fact that the boundary conditions are such that the solution will not be continuous throughout, but shocks will appear imbedded in the flow field. The method of characteristics is not capable of handling the appearance of shocks without appreciable complications.

The analysis proposed here specifically exploits the fact that the acoustic transit time is small acompared to the operation time $\bar{\tau}$. This is the situation in gas operated systems discussed so far; and the analysis is applicable for situations where the numerical computation by the method of characteristics becomes impractical.

With the $\bar{\ell}$ the characteristic length dimension, $\bar{\tau}$ the characteristic time and $\bar{a}_g(0)$ the characteristic velocity the following non-dimensional variables are introduced.*

$$\begin{aligned}
&1)\ \bar{t} = t\bar{\tau} && 9)\ \bar{F} = \bar{a}_g^{\,2}(0)F/\bar{\ell}\\
&2)\ \bar{x} = x\bar{\ell} && 10)\ \bar{q} = \bar{a}_g^{\,3}(0)q/\bar{\ell}\\
&3)\ \bar{u} = \bar{a}_g(0)u\\
&4)\ \bar{a} = \bar{a}_g(0)a\\
&5)\ \bar{p} = \bar{\rho}_g(0)\bar{a}_g^{\,2}(0)p\\
&6)\ \bar{\theta} = \bar{a}_g^{\,2}(0)\,\theta/\bar{R}_{gas} && (16)\\
&7)\ \bar{\rho} = \bar{\rho}_g(0)\rho\\
&8)\ \bar{h} = \bar{a}_g^{\,2}(0)h
\end{aligned}$$

*The sound velocity at $t = 0$ may indeed serve as reference velocity since the sound velocity $\bar{a}_g(\bar{t})$ is not a strong function of time $\bar{a}_g \sim (\bar{p}_g)^{(\gamma-1)/2\gamma}$ with $(\gamma-1)/2\gamma \ll 1$, where $\gamma \simeq 1.25$.

The differential equations then become

$$\varepsilon \frac{\partial \rho}{\partial x} + \frac{\partial (\rho u)}{\partial x} = 0 \tag{17}$$

$$\varepsilon \frac{\partial u}{\partial t} + u \frac{\partial u}{\partial x} + \frac{1}{\rho} \frac{\partial p}{\partial x} + F = 0 \tag{18}$$

$$-\varepsilon \frac{1}{\rho} \frac{\partial p}{\partial t} + \varepsilon \frac{\partial}{\partial t} \left(h + \frac{u^2}{2}\right) + u \frac{\partial}{\partial x} \left(h + \frac{u^2}{2}\right) - q = 0 \tag{19}$$

where $$\varepsilon \equiv \frac{\bar{\ell}}{\bar{\tau}\, \bar{a}_g(0)}$$

is the ratio of acoustic transit time to the flow duration time. We note here that the flow duration time $\bar{\tau}$ is of the same order as the average characteristic time $\overline{\bar{p}_g/(\partial \bar{p}_g/\partial \bar{t})}$, impressed on the flow in the duct by the time variation of the pressure in the barrel. Thus, we have

$$\bar{\tau} \sim 0\ (\bar{p}_g/[\partial \bar{p}_g/\partial \bar{t}]) \text{ with } \bar{\tau} >> \bar{\ell}/\bar{a}_g(0)$$

C. The Outer Problem

Since ε is a small number, we assume asymptotic expansions for the dependent variables of the form

$$\begin{aligned}
p\ (x,t;\varepsilon) &= p_1\ (x,t) + \delta_2\ (\varepsilon)\ p_2\ (x,t) + \ldots \\
\rho\ (x,t;\varepsilon) &= \rho_1\ (x,t) + \delta_2\ (\varepsilon)\ \rho_2\ (x,t) + \ldots \\
h\ (x,t;\varepsilon) &= h_1\ (x,t) + \delta_2\ (\varepsilon)\ h_2\ (x,t) + \ldots \\
u\ (x,t;\varepsilon) &= u_1\ (x,t) + \delta_2\ (\varepsilon)\ u_2\ (x,t) + \ldots
\end{aligned} \tag{20}$$

here $\dfrac{\delta_{n+1}(\varepsilon)}{\delta_n\ (\varepsilon)} \to 0$ in the limit $\varepsilon \to 0$ and $\delta_1\ (\varepsilon) = 1$ since the leading term for all expansions is of order unity.

Substituting these expansions into the full equations (17), (18), and (19) gives in the limit $\varepsilon \to 0$ the following set for the first order solution

$$\frac{\partial (\rho_1 u_1)}{\partial x} = 0$$

$$u_1 \frac{\partial u_1}{\partial x} + \frac{1}{\rho_1} \frac{\partial p_1}{\partial x} + F = 0 \qquad (21)$$

$$u_1 \frac{\partial}{\partial x} \left(h_1 + \frac{u_1^2}{2} \right) - q = 0$$

These equations are the equations describing the quasisteady flow; i.e., time appears in these equations only as a parameter. Consequently, the initial condition specified by (6) cannot be fulfilled by the solution to the above equations (21). This is a result of loss of the terms involving time derivative by the expansion process. The solution to (21) with the boundary condition (8) and (8a) cannot be uniformly valid in t because the initial conditions are violated. In order to obtain a uniformly valid solution another expansion for small t will be needed. This expansion will be given in Section III.D.

In the terminology of the method of matched asymptotic expansions the solution to (21) is called the outer solution, while the expansion for small $\bar{t}$ to be developed in Section III. D is called the inner solution. It will be shown later that both solutions can be matched and a composite solution can be found which is then a single expansion uniformly valid in $\bar{t}$.

Customarily, the variables pertaining to the outer solution are designated by small letters and those pertaining to the inner solution by capital letters. The subscript "1", designating the first approximation in the outer problem, will now be dropped.

The outer problem is that of a viscous heat conducting flow in a pipe of constant diameter. This is a problem of eminent practical importance and has been treated as early as 1875 (reference 5). Extensive discussions may be found in references 3, 6, and 7. Here, the treatment given in reference 6 will be followed, and only the main results quoted. For more detailed analysis the reader is referred to reference 6.

Using the notation

$$c_p \ \theta_{tot} = h_{tot} = h + \frac{u^2}{2}$$

the energy equation may be written as

$$u \frac{d\theta_{tot}}{dx} = q/c_p = q \ \bar{R}_{gas}/\bar{c}_p$$

with

$$q = -2f \frac{\bar{c}_p}{\bar{R}_{gas}} \frac{\bar{\ell}}{\bar{D}} (\theta_{tot} - \theta_w) \ u$$

we have

$$\frac{d\theta_{tot}}{dx} = - \frac{2 \ f \ \bar{\ell}}{\bar{D}} (\theta_{tot} - \theta_w) \qquad (22)$$

Since θ_w is assumed constant in x and t, this equation may be integrated with the boundary condition $\theta_{tot} = \theta_g$ at $x = 0$:

$$\theta_{tot} = \theta_w + (\theta_g - \theta_w) \cdot e^{-2f\bar{\ell}x/\bar{D}} \qquad (23)$$

Using (21) and the equation of state (5) one obtains with $M = u/a$ the following ordinary differential equation (see reference 6):

$$\frac{dM^2}{M^2} = \frac{(1 + \gamma M^2) \left(1 + \frac{\gamma-1}{2} M^2\right)}{(1 - M^2)} \frac{d \theta_{tot}}{\theta_{tot}} + \frac{\gamma M^2 \left(1 + \frac{\gamma-1}{2} M^2\right)}{(1 - M^2)} 4 \ f \frac{\bar{\ell}}{\bar{D}} dx \qquad (24)$$

Together with equation (22), this determines the Mach number distribution in the duct. This equation cannot be integrated in closed form and a numerical solution must be found. Once the Mach number, M, and the total temperature, θ_{tot}, are determined the other dependent variables can be found quite easily. The pertinent relations are provided later on.

First, the special case $\theta_{tot} >> \theta_w$ may be considered. In this case separation of variables is possible if θ_w is neglected in comparison with θ_{tot}. One then obtains from (24) and (22) the differential equation:

$$-\frac{dM^2}{M^2} = \frac{2\,f\,\bar{\ell}}{\bar{D}} \quad \frac{(1 + \frac{\gamma-1}{2}M^2)\,(1 - \gamma\,M^2)}{1 - M^2}\,dx \qquad (25)$$

This equation is readily integrated in closed form, though the solution is omitted here.

From the differential equation one notes the following condition for the sign of dM^2 for supersonic flow:

$$M^2 > 1\ ,\ dM^2 < 0$$

This means the Mach number always decreases if the initial Mach number at $\bar{x} = 0$ is supersonic. Mach number one is the limiting Mach number that can be reached on the supersonic branch and this Mach number is reached for a distance $\bar{x} = \bar{\ell}_{max}$ which is determined by the friction coefficient f, but which is quite small. If the duct length is larger than $\bar{\ell}_{max}$, then a shock occurs somewhere in the duct reducing the Mach number to subsonic values and the subsequent flow stays subsonic. For the subsonic flow:

$$\frac{1}{\gamma} < M^2 < 1,\quad dM^2 > 0$$

This means the Mach number increases in the direction of the flow. However, $M = 1$ cannot be surpassed and is reached only at the exit if $p_e > p_c$, since $dM^2/dx \to \infty$ as $M \to 1$ so that the inlet conditions are adjusted to allow $M = 1$ to occur only at the exit. For $p_c = p_e$ the flow is subsonic at the exit also. The lower limit at $1/\gamma$ is a consequence of the special assumption of $\theta_w = 0$. For $M^2 = 1/\gamma$ at $x = 0$, the Mach

number stays constant in the duct since $dM^2/dx = 0$. Below this value $dM^2 < 0$, i.e.: the Mach number decreases. As equation (23) shows, the condition $\theta_w << \theta_{tot}$ is not a valid assumption for the specific case of the M-16 rifle, but could be a good assumption for a different application. For the general case θ_w is finite, then the Mach number in the subsonic branch first decreases and then increases reaching the condition $dM^2/dx = 0$ only for one value of x, which, of course, gives the minimum value of M. M = 1 is here reached only at the exit for $p_e > p_c$; for $p_e = p_c$ only subsonic flow can occur at the exit. The supersonic branch has the same qualitative behavior as above. The phenomenon discussed above is termed "choking" because it gives a limitation on the maximum mass flow. The conditions for choking in the general case are difficult to state but a lucid physical interpretation is given by Prandtl[7] for the case of zero heat transfer.

Figure 3 shows the Mach number distribution along x from numerical computations for the general case of θ_w finite. Shown also is the location of the shock. For a given Mach number distribution in the supersonic branch, say $M_I = f(x)$, and a given Mach number distribution for the subsonic branch, say $M_{II} = g(x)$, the location of the shock x_s is uniquely determined by the condition:

$$M_I^2 = \left(M_{II}^2 + \frac{2}{\gamma-1}\right) \Big/ \left(\frac{2\gamma}{\gamma-1} M_{II}^2 - 1\right) \qquad (26)$$

For increasing shock strength, the shock moves closer to the nozzle and eventually vanishes in the nozzle, i.e., $x_s \to 0$; this occurs when no pair of Mach numbers can be found to fulfill the relation (26). In this case, to be discussed later, a shock may still occur in the nozzle.

For the supersonic branch $M_I = f(x)$ results from integrating equation (24) with the boundary condition: $M = M_p$ at $x = 0$, where M_p (> 1) is given from the area ratio of the nozzle by:

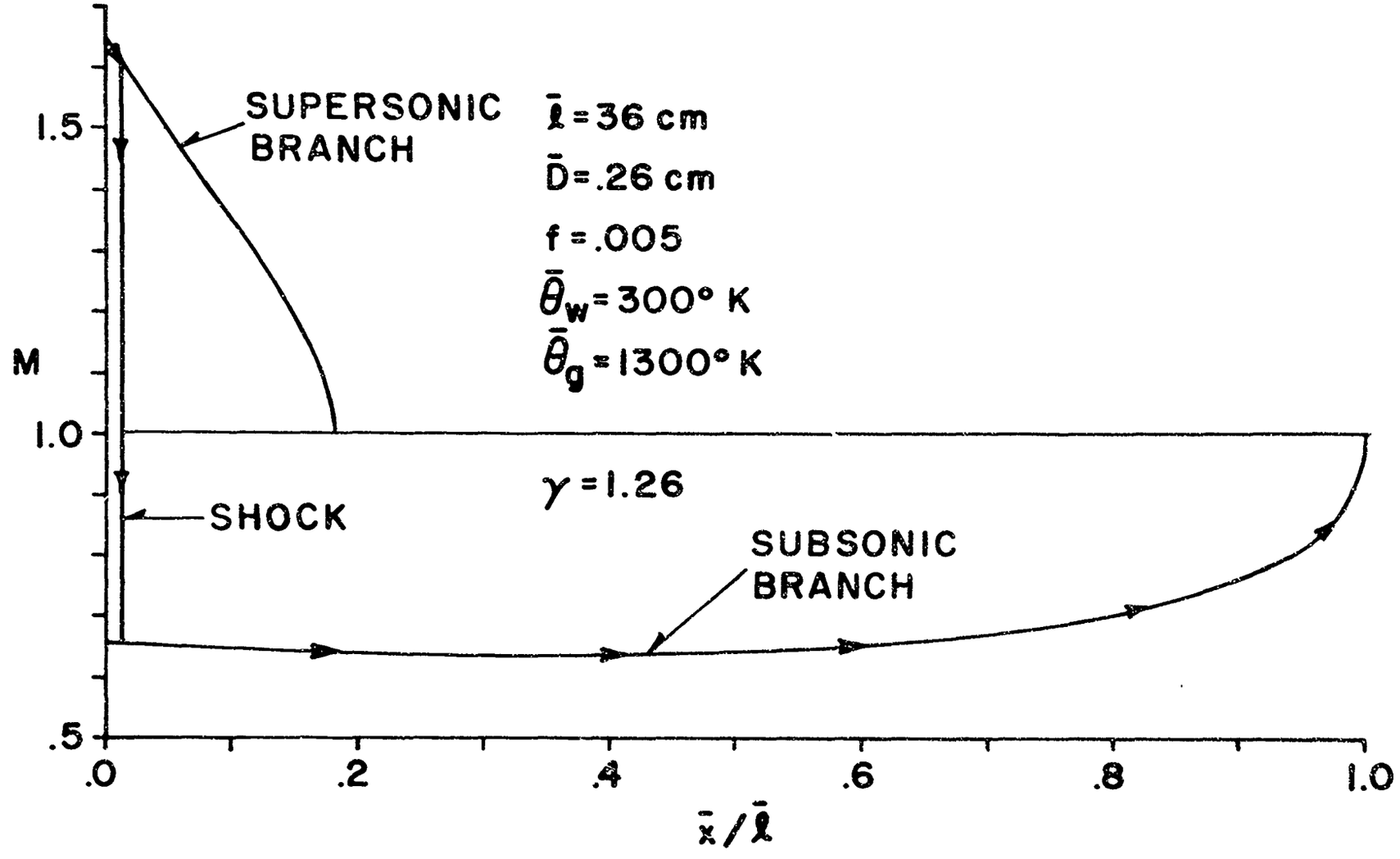

Figure 3. Outer Solution Variation of Mach Number in Gas Tube

$$\omega \equiv \frac{\bar{A}_p}{\bar{A}_{min}} = \frac{1}{M_p}\left[\frac{2}{\gamma+1}\left(1 + \frac{\gamma-1}{2} M_p^2\right)\right]^{\frac{\gamma+1}{2(\gamma-1)}} \tag{27}$$

The subsonic branch $M_{II} = g(x)$ is obtained by integrating equation (24) with the boundary condition

$$x = 1: \quad M = M_e = 1 \quad \text{for } p_e > p_c$$

For $p_e = p_c$, neither M_e nor M_{II} is known beforehand, but must be determined by an iterative process. First, equation (24) is integrated for various values of $M_e < 1$, thus giving a set of value pairs $M_{II} = F(M_e)$. Another relation between M_{II} and M_e is readily found from the continuity equation and the thermal equation of state

$$\frac{p_e}{p_{II}(x_s)} = \frac{p_c}{p_{II}(x_s)} = \frac{M_{II}}{M_e}\left(\frac{\theta_e}{\theta_{II}}\right)^{1/2} \tag{28}$$

Here, the index II designates the quantity on the subsonic side of the shock at the location x_s. For the "no shock" condition $x_s = 0$ and $p_{II}(0) = p_p$. In any case, $p_{II}(x_s)$ can be uniquely related to p_p and, thus, to p_g as will be shown below. The ratio of static temperatures follows from the energy equation:

$$\frac{\theta_e}{\theta_{II}} = \frac{\theta_{e\,tot}}{\theta_{II\,tot}} \frac{1 + \frac{\gamma-1}{2} M_{II}^2}{1 + \frac{\gamma-1}{2} M_e^2} \tag{29}$$

This relation is valid for any station x, i.e., for any index, whether a shock occurs or not. Since p_c and p_g are given for each step in the parameter t, equation (28) is another relation of the form $M_{II} = G(M_e)$. The two relations $M_{II} = F(M_e)$ and $M_{II} = G(M_e)$ can be solved numerically for M_{II} and M_e.

With M_e known the other variables with the subscript e are readily found. These variables are used in obtaining the inhomogeneous terms in the differential equations for the cavity flow in Section III.A and are functions of the parameter t.

The state with the index e relates to the state on the subsonic side of the shock by:

$$\frac{p_e}{p_{II}} = \frac{M_{II}}{M_e}\left[\frac{\theta_e}{\theta_{II}(x_s)}\right]^{1/2}$$

$$\frac{u_e}{u_{II}} = \frac{M_e}{M_{II}}\left[\frac{\theta_e}{\theta_{II}(x_s)}\right]^{1/2} \qquad (30)$$

$$\frac{\rho_e}{\rho_{II}} = \frac{p_e}{p_{II}}\,\frac{\theta_{II}(x_s)}{\theta_e}$$

The normal shock relations connect state I with state II and are given here for completeness:

$$\frac{p_{II}}{p_I} = \frac{2\gamma\, M_I^2 - (\gamma-1)}{\gamma+1}$$

$$\frac{\rho_{II}}{\rho_I} = \frac{(\gamma+1)\, M_I^2}{(\gamma-1)\, M_I^2 + 2} \qquad (31)$$

The state I is connected to state p by equations analogous to equation (30).

$$\frac{p_I(x_s)}{p_p} = \frac{M_p}{M_I(x_s)}\left[\frac{\theta_I(x_s)}{\theta_p}\right]^{1/2}$$

$$\frac{u_I(x_s)}{u_p} = \frac{M_I(x_s)}{M_p}\left[\frac{\theta_I(x_s)}{\theta_p}\right]^{1/2} \qquad (32)$$

$$\frac{\rho_I(x_s)}{\rho_p} = \frac{p_I(x_s)}{p_p}\,\frac{\theta_p}{\theta_I(x_s)}$$

$\theta_I(x_s)/\theta_p$ is given by

$$\frac{\Theta_I(x_s)}{\Theta_p} = \frac{\Theta_{I\,tot}}{\Theta_g} \quad \frac{1 + \frac{\gamma-1}{2} M_p^2}{1 + \frac{\gamma-1}{2} M_I^2} \tag{33}$$

If no shock occurs in the duct the state e or any other state x is related to state p immediately by equations of the form (30). These equations provide all the variables at the entrance of the cavity for all times except for very early times where the quasisteady approximation is invalid.

Keeping in mind that the very short nozzle is considered frictionless, the variables with the index g and p are related by the following if $M_p > 1$:

$$\begin{aligned}
\Theta_g/\Theta_p &= 1 + \frac{\gamma-1}{2} M_p^2 \\
p_g/p_p &= (1 + \frac{\gamma-1}{2} M_p^2)^{\gamma/(\gamma-1)} \\
\rho_g/\rho_p &= (1 + \frac{\gamma-1}{2} M_p^2)^{1/(\gamma-1)} \qquad (34) \\
\Theta_p &= p_p/\rho_p \\
u_p &= M_p (\gamma p_p/\rho_p)^{1/2}
\end{aligned}$$

If no shock can be found in the duct then $M_p < 1$, but a shock may still occur in the nozzle. This is the case where M_p is too large to give a purely subsonic flow in the nozzle. The limiting $M_{p\,lim}$ may be computed from equation (27) which also allows a subsonic solution. For any Mach number $1 > M_p > M_{p\,lim}$ there occurs a shock in the nozzle. The density ρ_p may be computed from

$$\rho_p = \rho_g \left(\frac{2}{\gamma+1}\right)^{1/(\gamma-1)} (\omega M_p)^{-1} \left[\frac{2}{(\gamma+1)} (1 + \frac{\gamma-1}{2} M_p^2)\right]^{-1/2} \tag{35}$$

and the temperature θ_p is

$$\theta_p = \theta_g \left[1 + (\gamma-1)\, M_p^2/2\right]^{-1}$$

Together with the equation of state (5) these relations determine the conditions at state p for this case.

If $M_p < M_{p\,lim}$ the flow in the nozzle is purely subsonic. Experiments suggest that then the pressure loss due to the sudden area increase between port and duct must be included. The three conservation equations of mass, energy, and momentum applied between the station p and the throat (*quantities) lead to the relation (Appendix A)

$$M^{*2} = \frac{1}{2}\left[-1 + 2\gamma\, G\omega + \sqrt{1 - 4\, G\omega\, (\gamma - \frac{\gamma-1}{2}\,\omega)}\right]\left(\frac{\gamma-1}{2} - G\gamma^2\right)^{-1} \qquad (36)$$

with $G = M_p^2\,(1 + \frac{\gamma-1}{2}\,M_p^2)\,(\gamma M_p^2 + 1)^{-2}$

This equation gives M^*, and the other variables follow from

$$p^* = p_g\,(1 + \frac{\gamma-1}{2}\,M^{*2})^{-\gamma/\gamma-1}$$

$$\theta^* = \theta_g\,(1 + \frac{\gamma-1}{2}\,M^{*2})^{-1}$$

$$\rho^* = (\theta^*)^{-1}\, p^*$$

$$u^* = M^*\,(\gamma\,\theta^*)^{1/2} \qquad (37)$$

and further

$$p_p = \frac{p^*}{\omega}\,\frac{M^*}{M_p}\,\left(\frac{\theta_p}{\theta^*}\right)^{1/2}$$

$$\theta_p = \theta^*\,(1 + \frac{\gamma-1}{2}\,M^{*2})\;\;(1 + \frac{\gamma-1}{2}\,M_p^2)^{-1}$$

$$u_p = M_p\,(\gamma\,\theta_p)^{1/2}$$

The condition $p_c > p_g$ may occur and in this case there is back flow from the cavity to the barrel. This back flow occurs with $p_c - p_g << p_c$ so that the effect of pressure on the density may be neglected, i.e., $p \neq \text{fn}\ (\rho)$. However, the effect of temperature on the density may have to be considered.

From equation (21) and conservation of mass and momentum applied across the discontinuities, there follows for the backward flow in accordance with Figure 4*

$$u_{e''}^2 = \frac{2(p_c - p_g)}{\rho_c\left[\left(\frac{1}{\alpha_e} - 1\right)^2 + \omega^2\left[1 + \left(\frac{1}{\alpha_p} - 1\right)^2\right] + \frac{4f\bar{\ell}}{\bar{D}}\right]} \tag{38}$$

Here α_e and α_p are contraction coefficients. These are a strong function of the Mach number with $\alpha_e \approx 0.62$ for incompressible flow (M = 0) and $\alpha_e = 1.0$ for M = 1. α_p is also a function of ω. For the compressible flow the contraction coefficients have seen set equal to 1.**

The coefficient f includes losses due to bends as well as the friction in the duct and is given by

$$f = [\bar{D}/(4\bar{\ell})]\ (K_F + K_B) \tag{39}$$

The pressure at station e" is related to the pressure in the cavity by

$$p_c - p_{e''} = \frac{\rho_e}{2} u_{e''}^2 \left[\left(\frac{1}{\alpha_e} - 1\right)^2 + 1\right] \tag{40}$$

with $\Theta_{e''} \approx \Theta_c$, $\rho_{e''} \approx \rho_c$, and where $p_{e''} \rightarrow p_e$, etc., in equations (1), (2), (3).

The later phases of the forward flow may also be computed using $p \neq \text{fn}\ (\rho)$ but $\rho = \text{fn}\ (\theta)$.

$$u_e^2 = 2\ (\Theta_{e\ tot}/\Theta_g)^2\ (p_g - p_c)\ \rho_g^{-1}\left[\left(\frac{\omega}{\alpha_g} - \omega\right)^2 + (\omega-1)^2 - 1 + 2\,\frac{\Theta_{e\ tot}}{\Theta_g} + \frac{4f\bar{\ell}}{\bar{D}\Theta_g}\int_0^1 \Theta dx\right]^{-1} \tag{41}$$

* Derivation in Appendix B

**For $\rho \neq \text{fn}\ (\theta)$, the assumption $p \neq \text{fn}\ (\rho)$ gives incompressible flow.

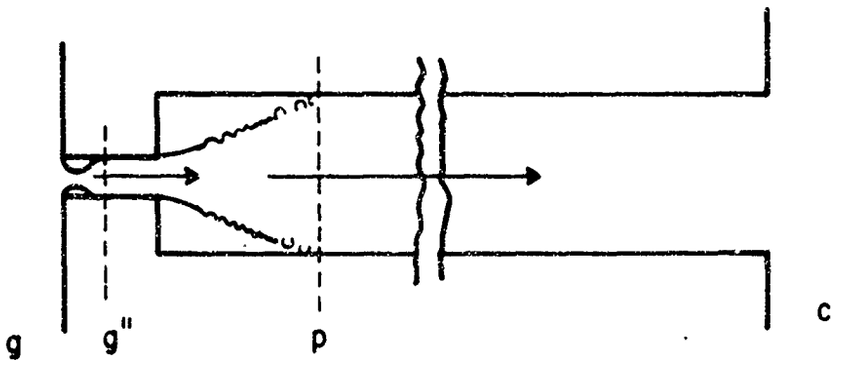

a) Forward Flow

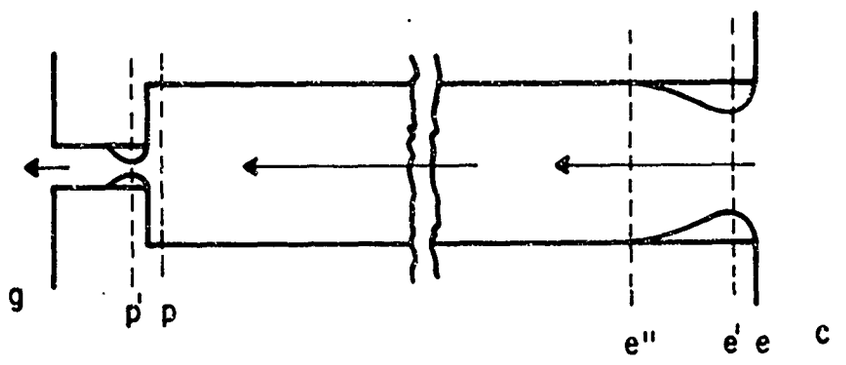

b) Backward Flow

Figure 4. Sketch for Derivation of Approximate Flow Relations

$$\frac{1}{\theta_g}\int_0^1 \theta \, d\,x = \frac{\theta_w}{\theta_g} + \left(2f\frac{\bar{\ell}}{\bar{D}}\right)^{-1}\left(1 - \frac{\theta_w}{\theta_g}\right)\left(1 - e^{-2f\bar{\ell}/\bar{D}}\right) \qquad (42)$$

The coefficients α_p, α_e, α_g, and K_F and K_B are listed in Table 3.

D. The Inner Problem

As mentioned earlier the solution given in Section III.C is not uniformly valid in t and fails for small t. This singular behavior is a result of loss of the time derivative in the differential equation by the expansion procedure. The nonuniformity occurs near the line t = 0 and in order to investigate this region a magnified variable T is introduced. The variable x remains unchanged since the quasisteady solution behaves regularly here. The dependent variables in the earlier times are of the same order as for the later times and also remain unaltered. Thus,

$$T = t/\delta(\varepsilon) \qquad U = u \qquad \Omega = \rho$$

$$X = x \qquad P = p \qquad H = h$$

$$\Lambda = a$$

Introducing these variables into the differential equations (17), (18), and (19) gives

$$\frac{\varepsilon}{\delta(\varepsilon)}\frac{\partial \Omega}{\partial T} + \frac{\partial(\Omega U)}{\partial X} = 0$$

$$\frac{\varepsilon}{\delta(\varepsilon)}\frac{\partial U}{\partial T} + U\frac{\partial U}{\partial X} + \frac{1}{\Omega}\frac{\partial P}{\partial X} = 0 \qquad (43)$$

$$\frac{\varepsilon}{\delta(\varepsilon)}\frac{\partial}{\partial T}\left(H + \frac{U^2}{2}\right) + U\frac{\partial}{\partial X}\left(H + \frac{U^2}{2}\right) - \frac{\varepsilon}{\delta(\varepsilon)}\frac{\partial P}{\partial T} = 0$$

where we have dropped the friction and heat transfer terms in accordance with the discussion in Section II. In the limit $\varepsilon \to 0$, $\varepsilon/\delta(\varepsilon) \to 0$

results again in the loss of the highest derivative, while $\varepsilon/\delta(\varepsilon) \to \infty$ when $\varepsilon \to 0$ leads to a solution which cannot be matched with the outer solution. Thus, we must have

$$\frac{\varepsilon}{\delta(\varepsilon)} \to \text{const. as } \varepsilon \to 0 \quad .$$

Without loss of generality the constant is taken equal to 1; thus, we have $\delta(\varepsilon) = \varepsilon$, and we get the differential equations

$$\frac{\partial \Omega}{\partial T} + \frac{\partial(\Omega U)}{\partial X} = 0$$

$$\frac{\partial U}{\partial T} + U \frac{\partial U}{\partial X} + \frac{1}{\Omega} \frac{\partial P}{\partial X} = 0 \qquad (44)$$

$$\frac{\partial}{\partial T} \left(H + \frac{U^2}{2}\right) + U \frac{\partial}{\partial X} \left(H + \frac{U^2}{2}\right) - \frac{\partial P}{\partial T} = 0$$

with the initial conditions

$$T = 0, \quad X > 0: \quad P = P_i; \quad \Lambda = \Lambda_i; \quad U = 0$$

$$X < 0: \quad P = P_g; \quad \Lambda = \Lambda_g; \quad U = 0 \quad .$$

The boundary conditions for $T > 0$ are those existing at the edge of the region of nonuniformity.

$$X = 0, \quad T > 0: \quad P(0,T) = \lim_{t \to 0} p(0,t), \quad \Lambda(0,T) = \lim_{t \to 0} a(0,t),$$

$$U(0,T) = \lim_{t \to 0} u(0,t)$$

For $X = 1$ no boundary condition is applied as long as $U_e > \Lambda_e$; and for $U_e < \Lambda_e$ the condition is

$$T > 0, \quad X = 1: \quad P(1,T) = \lim_{t \to 0} p_c(t) = p_i \quad .$$

There is no continuous solution satisfying these initial and boundary conditions and the actual solution contains surfaces of discontinuities. A solution is readily constructed using shock wave, contact front, uniform region of flow, unsteady expansion and steady expansion. The problem is that of a shock tube having an area change at the diaphragm station.[8,9,10]

Figure 5 shows an X,T diagram of the flow in the customary shock tube notation. Since one is interested in the influx of powder gas into the cavity one may neglect the gas between shock and contact front, which is, of course, the gas (air) contained in the tube at time $t < 0$, and is not powder gas.

With $U_2 = U_3$ across the contact front we set $U_e = 0$ for $T < U_2^{-1}$.

In the region 3 we have constant flow properties. Thus,

$$U_e = U_3 = U_2 = \text{const.} \qquad \text{for} \qquad U_2^{-1} \leq T \leq \left[U_2 \frac{\gamma+1}{2} - (\gamma-1)\, R\right]^{-1}$$

where $2R \equiv U_p + \frac{2}{\gamma-1} \Lambda_p = \text{Const.}\ (= U_{3'} + \frac{2}{\gamma-1} \Lambda_{3'})$ is the Riemann invariant. The pressure across the contact front is equal so that $P_2 = P_3$.

P_e follows from the shock relation (31). For $M_s >> 1$ we have

$$P_e/P_i = P_2/P_1 \approx \frac{2\hat{\gamma}}{\hat{\gamma}+1} M_s^2, \qquad (M_s \equiv U_s/\Lambda_1)$$

and rewriting this expression in terms of U_2:

$$P_2/P_1 \approx \left(\frac{U_2}{\Lambda_1}\right)^2 \frac{\hat{\gamma}\,(\hat{\gamma}+1)}{2} \tag{45}$$

U_2 may be found by numerically solving [8]

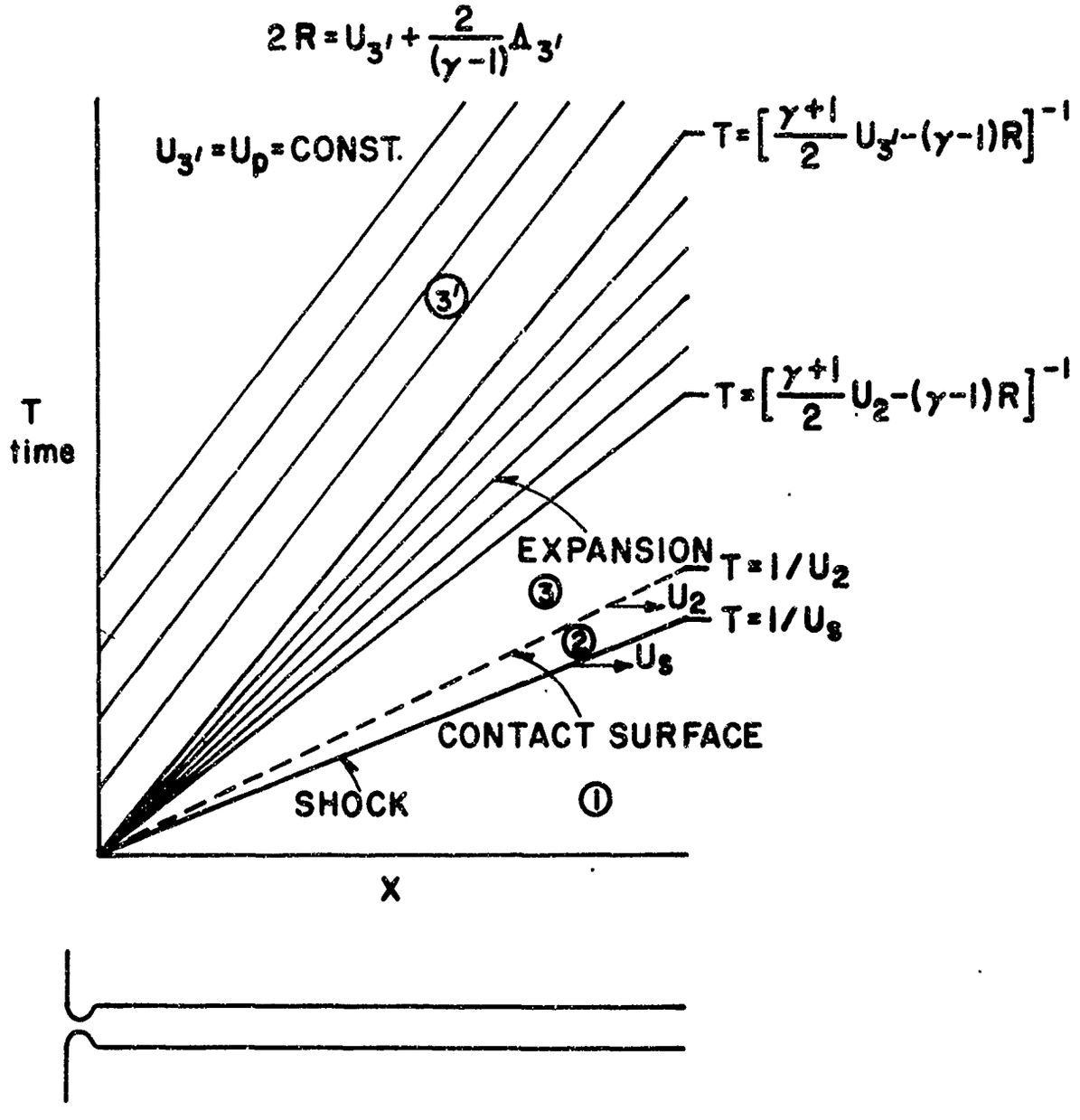

Figure 5. X, T Diagram for Inner Solution--Nozzle at Port

$$\frac{P_g(0)}{P_1} \approx \left(\frac{U_2}{\Lambda_1}\right)^2 \frac{\hat{\gamma}(\hat{\gamma}+1)}{2g}\left[1 - \frac{U_2}{\Lambda_g(0)}\frac{\gamma-1}{2} g^{-\frac{\gamma-1}{2\gamma}}\right]^{-\frac{2\gamma}{\gamma-1}} \qquad (46)$$

Here, $\hat{\gamma} = 1.4$ and the gain factor g is

$$g = \left\{\left[\frac{2}{2 + (\gamma-1) M_{3'}^2}\right]^{1/2} \left[\frac{2 + (\gamma-1) M_{3'}}{2}\right]\right\}^{2\gamma/(\gamma-1)},$$

where $M_{3'} = M_p$ from equation (27). Flow variables at state 3′ are found from equation (34).

$$\Omega_e/\Omega_p = \Omega_3/\Omega_{3'} \approx \left[\frac{\hat{\gamma}(\hat{\gamma}+1)}{2}\left(\frac{U_2}{\Lambda_1}\right)^2 \frac{P_1}{P_{3'}}\right]^{1/\gamma} . \qquad (47)$$

It is emphasized that constant flow properties in this region are a result of neglecting heat transfer and friction and also shock reflections; actually, these variables depend on Reynolds number, geometry and time.

The flow properties in the expansion fan depend on T for X = 1.

Thus, for:

$$\left[U_2 \frac{\gamma+1}{2} - (\gamma-1) R\right]^{-1} \leq T \leq \left[U_{3'} \frac{\gamma+1}{2} - (\gamma-1) R\right]^{-1}$$

we have

$$U(1,T) = \frac{\gamma-1}{\gamma+1} 2R + \frac{2}{\gamma+1}\frac{1}{T}$$

$$P(1,T) = P_{3'}\left[\frac{1}{\Lambda_{3'}}\frac{\gamma-1}{\gamma+1}\left(2R - \frac{1}{T}\right)\right]^{\frac{2\gamma}{\gamma-1}} \qquad (48)$$

$$\Lambda(1,T) = \frac{\gamma-1}{\gamma+1}\left(2R - \frac{1}{T}\right)$$

For time

$$\left[U_{3'} \frac{\gamma+1}{2} - (\gamma-1) R \right]^{-1} \leq T \leq \infty$$

the flow properties are constant

$$U(1,T) = U_p = U_{3'} \quad \Lambda(1,T) = \Lambda_p = \Lambda_{3'}$$
$$P(1,T) = P_p = P_{3'} \tag{49}$$

E. The Composite Solution for the Flow in the Duct

The analysis described so far has yielded the first terms of two complementary asymptotic expansions. In general the two asymptotic expansions valid for small and large times respectively have a domain of overlap, in which both are valid. This is the case whenever Van Dyke's"asymptotic matching principle" is valid. This principle applied here amounts to setting the first term inner expansion of the first term outer expansion (the outer expansion rewritten in inner variables and expanded for small ϵ truncated to the first term) equal to the first term outer expansion of the first term inner expansion. This principle leads, for the velocity, to the condition

$$U(X,\infty) = u(x,0) \tag{50}$$

with corresponding expressions for the other dependent variables. We note that from equation (49)

$$U(1,\infty) \equiv U_e(\infty) = U_{3'} = U_p$$

For inviscid and nonheat-conducting flow the solution to equation (21) is trivial and gives

$$\mathbf{u}(x;\, t)_{\text{invisc}} = u_p(t)_{\text{invisc}} = u_e(t)_{\text{invisc}} = \text{const.}$$

where the constant is a function of the parameter t.

For $t = 0$ we have

$$u(x,0)_{invisc} = u_{p\ invisc}(0) \equiv U(1,\infty)$$

so that the matching condition is fulfilled for inviscid flow. In this case the two solutions may be combined to yield one composite solution, which then is uniformly valid over the whole range of t.

Using the multiplicative composition of reference 11, one finds the composite expansion as the outer expansion multiplied by a correction factor consisting of the ratio of the inner expansion to its outer expansion.

$$u_{comp.} = u(1,t)\ \frac{U(1,T)}{U(1,\infty)} \tag{51}$$

Since in the present case the outer solution has been computed on the basis of viscous heat-conducting flow, matching of the inner and outer solutions is not immediately possible for $x > 0$. For $x = 0$ and supersonic flow at the entrance of the duct, matching of the inner and outer solution according to equation (50) is effected; for subsonic flow matching is not possible, reflecting the fact that the disturbances due to friction now affect the entrance condition in the duct. Failure to match according to (50) of course simply represents the fact that the inner and outer solutions are different approximations in the parameter 1/Re.

Formally the composite solution of the form (51) may be used here also. The effect of friction and heat transfer on the velocity may be assumed accounted for in the following way:

$$U(1,T)_{visc} = \beta\ U(1,T) \tag{52}$$

where the factor β will depend on Reynolds number, geometry, Mach Number and pressure ratio and on time. The composite solution will be

$$u_{comp.,\ e} = u(1,t)\ \frac{U(1,t/\varepsilon)}{U(1,\infty)}\ \frac{\beta(t/\varepsilon)}{\beta(\infty)} \tag{53}$$

For $t/\varepsilon < (U_2\beta)^{-1}$, $u_{comp.} = 0$ because $U_e = 0$. This time $\bar{t} = \varepsilon\ \bar{\tau}\ (\bar{U}_2\beta)^{-1} = \bar{\ell}\ (\bar{U}_2\beta)^{-1}$ is of course the delay time between rise of

pressure at the port and rise of pressure in the cavity. This time has been observed experimentally; it determines $\tilde{\beta}$, the average value of β in the range $0 < \bar{t} < \bar{\ell}\ (\bar{U}_2\tilde{\beta})^{-1}$. The experimental values of $\tilde{\beta}$ scatter between 1 and 0.5.

For $\bar{t} = \infty$ one can find from the matching condition, when applied to viscous flow, $\beta\ (\infty)$ as

$$\beta\ (\infty) = u(1,0) \,/\, U(1,\infty),$$

and this leads to a numerical value of $\beta \approx 0.35$. Since $\beta(\bar{t})$ is expected to vary quite rapidly near $\bar{t} = 0$, it is assumed that at the end of the first interval, i.e., at $\bar{t} = \bar{\ell}\ (\bar{U}_2\tilde{\beta})^{-1}$, β has essentially reached the value for $\bar{t} \to \infty$; thus we set the ratio $\beta\ (t/\varepsilon) \,/\, \beta\ (\infty) \approx 1$.

The ratio $\beta\ (t/\varepsilon) \,/\, \beta\ (\infty)$ can also be considered an adjustable parameter with which the computation could be adjusted so as to give best agreement with experiment. This is not done here since this procedure could disguise other phenomena. It is not possible to correctly account for the friction and heat transfer at the very early times, as has been pointed out before, and some sort of plausible assumption has to be made. The basic difficulty is that the equations (13) and (14) with the quasisteady friction and heat transfer coefficients are not applicable in this early phase; and the treatment of this problem, say, by the method of characteristics would of course not remove this difficulty.

With the assumption that the viscous correction factor for velocity $\beta(t/\varepsilon) \,/\, \beta(\infty) \approx 1$ for $\bar{t} > \bar{\ell}\ (U_2\tilde{\beta})^{-1}$ and that the corresponding correction factors for the other variables are also approximately unity, the effect of friction appears only in the delay time $\bar{t} = \bar{\ell}\ (\bar{U}_2\tilde{\beta})^{-1}$, where it can be observed experimentally, and in the other interval boundaries, where it cannot be directly observed.

The composite solution in the appropriate intervals is then

$$\bar{u}_{comp,\,e} = 0,$$

for $0 < \bar{t} < \bar{\ell}(\bar{U}_2\tilde{\beta})^{-1}$

$$\bar{u}_{comp,e} = \bar{u}(\bar{\ell};\,\bar{t})\;\bar{U}_2/\bar{U}_3,$$

for $\bar{\ell}\;(\bar{U}_2\tilde{\beta})^{-1} < \bar{t} < \bar{\ell} \;/\; [\bar{U}_2\;(\frac{\gamma+1}{2}) - (\gamma-1)\;\bar{R}]\tilde{\beta}$

$$\bar{u}_{comp,e} = \bar{u}\;(\bar{\ell};t)\;(\frac{\gamma-1}{\gamma+1}\,2\bar{R} + \frac{2}{\gamma+1}\;\frac{\bar{\ell}}{\bar{t}})\;\bar{U}_3^{-1} \qquad (54)$$

for $\bar{\ell} \;/\; [\bar{U}_2\;\frac{\gamma+1}{2} - (\gamma-1)\bar{R}\;]\;\tilde{\beta} < t < \bar{\ell} \;/\; [\bar{U}_3\;\frac{\gamma+1}{2} - (\gamma-1)\bar{R}]\;\tilde{\beta}$

$$\bar{u}_{comp,\,e} = \bar{u}\;(\bar{\ell};\bar{t})$$

for $\bar{\ell}\;/[\bar{U}_3\;(\frac{\gamma+1}{2}) - (\gamma-1)\;\bar{R}]\;\tilde{\beta} < \bar{t} < \infty$.

It has been assumed here for simplicity that β for the Riemann invariant is the same as β for the velocity. This assumption is quite acceptable within the assumptions made already and can only result in a slight shift in the interval boundaries. It should be remembered that the time after which the effect of the first phase has completely died out is $\bar{t} = \bar{\ell} \;/\; [\bar{U}_3\;(\frac{\gamma+1}{2}) - (\gamma-1)\;\bar{R}]\;\tilde{\beta}$, and that this time is still small compared to $\bar{\tau}$.

The composite solution for the pressure in the corresponding intervals is:

$$\bar{p}_{comp,\,e} = \bar{p}_e(\bar{\ell};\bar{t})\;\bar{P}_1/\bar{P}_3,$$

$$\bar{p}_{comp,\,e} = \bar{p}_e(\bar{\ell};\bar{t})\;\bar{P}_2/\bar{P}_3,$$

$$\bar{p}_{comp,\,e} = \bar{p}_e(\bar{\ell};\bar{t})\;\left[\frac{1}{\bar{A}_3}\;\frac{\gamma-1}{\gamma+1}\;(2\;\bar{R} - \frac{\bar{\ell}}{\bar{t}})\right]^{2\gamma/(\gamma-1)} \qquad (55)$$

$$\bar{p}_{comp,e} = \bar{p}_e(\bar{\ell};\bar{t})$$

Similarly for the sound speed

$$\bar{a}_{comp.,\,e} = \bar{a}_e\,(\bar{\ell};\bar{t})\;\bar{\Lambda}_1/\bar{\Lambda}_{\cdot}$$

$$\bar{a}_{comp.,\,e} = \bar{a}_e\,(\bar{\ell};\bar{t})\;(\bar{P}_2/\bar{P}_{3\cdot})^{(\gamma-1)/2\gamma} \qquad (56)$$

$$\bar{a}_{comp.,\,e} = \bar{a}_e(\bar{\ell};\bar{t})\left[\frac{\gamma-1}{\gamma+1}\,(2\,\bar{R} - \frac{\bar{\ell}}{\bar{t}}\,)\right] / \bar{\Lambda}_{3\cdot}$$

$$\bar{a}_{comp.,\,e} = \bar{a}_e(\bar{\ell};\bar{t})$$

The composite solutions given by equations (54), (55), and (56) provide $\bar{u}_e$, $\bar{p}_e$, and $\bar{a}_e$ for equations (1), (2), and (3). The other dependent variables at the cavity entrance (location e) may be computed from these quantities.

IV. COMPARISON WITH EXPERIMENT

A comparison between theory and experiment was made on the M-16 Rifle. Input data for the theoretical computation consist of the measured time variable pressure in the barrel at the port location, the physical properties of the powder gas, and the dimensions of the gas system. The physical properties of the powder gas are listed in Table 1. They represent estimates based on the interior ballistics*

Table 1. Properties of Powder Gas

$\bar{c}_p$	$= 1.74 \times 10^3$ (m/sec)^2/°K
$\bar{c}_v$	$= 1.38 \times 10^3$ (m/sec)^2/°K
$\bar{k}$	$= 0.831 \times 10^{-1}$ (kg m)/(sec^3 °K)
$\bar{R}_{gas}$	$= 0.400 \times 10^3$ (m/sec)^2/°K
γ	$= 1.26$
$\bar{\gamma}$	$= 1.24$
$\bar{\mu}$	$= 4.80 \times 10^{-5}$ kg/(m sec)

*Supplied by Mr. R. Geene, of Interior Ballistics Laboratory

computation of the composition of the powder gas. The dimensions of the gas system are summarized in Table 2.*

Table 2. Dimensions of Gas System

$\bar{A} = 1.269 \times 10^{-4}\ m^2$

$\bar{A}_e = 0.6605 \times 10^{-5}\ m^2$

$\bar{A}_{min} = 0.4383 \times 10^{-5}\ m^2$

$\bar{A}_p = 0.6605 \times 10^{-5}\ m^2$

$\bar{A}_v = 0.6533 \times 10^{-5}\ m^2$

$\bar{D} = 0.2900 \times 10^{-2}\ m$

$\bar{\ell} = 0.3600\ m$

$\bar{M}_B = 0.4366\ kg$

$\bar{r}_v = 0.1442 \times 10^{-2}\ m$

$\bar{V}_{ci} = 0.7600 \times 10^{-6}\ m^3$

$\bar{x}_{BE} = 0.7600 \times 10^{-2}\ m$

$\bar{x}_{Bv} = 0.6158 \times 10^{-2}\ m$

$(\bar{\epsilon}/\bar{D}) \approx 0.015$

Since it is necessary to specify another variable of state at the port, the temperature at the port was computed according to:

$$\theta(t)/\theta(0) = \left[p(t)/p(0) \right]^{(\tilde{\gamma}-1)/\tilde{\gamma}} \qquad (57)$$

Here $\tilde{\gamma}$ is not the ratio of specific heats, but an exponent determined by fitting the temperature variation, known from the standard interior ballistic treatment of the weapon, to the pressure variation according to equation (57). The standard interior ballistics treatment breaks down after the bullet has left the barrel; the temperature distribution, however, is needed for the computation after this time, and is extrapolated according to equation (57).

*Supplied by Mr. M. Werner of Interior Ballistics Laboratory.

Probably the largest uncertainties lie in the various loss factors. For the friction factor the value for clean commercial steel pipe has been used.[12] Compressibility effects on the friction are apparently quite small, at least for hydraulically smooth pipes where Frossel[7] did not find any dependence on the Mach number of the flow. For rough pipes such as the commercially clean pipe used as duct in the M-16 rifle, (relative roughness $\bar{\epsilon}/\bar{D} \approx 0.015$) the dependence of the friction factor on Mach number is probably more pronounced, and will result in a slightly smaller friction factor. Since during the time $\bar{\tau}$ the flow in the duct ranges from supersonic to subsonic and incompressible flow, the friction factor could be introduced as depending on the Mach number. This has, however, not been done; the friction factor is assumed to be constant at the value for incompressible flow. It may be mentioned that the experimental work[2] was conducted with a used rifle showing evidence of deposits in the interior of the duct. X-ray pictures of ducts in the M-16 rifle show indeed substantial amounts of deposits depending on powder type and usage of the rifle.[13] The deposits are so located as to cause little additional resistance in forward flow where stagnation pressure is high, but in the backward flow they may cause a considerable increase in losses.

The losses due to bends are taken into account by loss coefficients as is done in incompressible flows. The loss coefficients are taken from reference 12. The losses apply to miter bends, which are most representative of the bends in the gas duct system. Again, compressibility effects probably tend to decrease the losses slightly.

The area reduction at the port has been treated as a frictionless nozzle for supercritical pressure ratios and as an abrupt area change for subcritical pressure ratios as is explained in Section III. In the Addendum the analysis has been extended to include treatment of the area reduction as an abrupt area change even for the case of supercritical pressure ratios. In this case supersonic flow cannot be reached in the duct. It is not possible to decide which of the two types of flows is actually established, because, as will be shown, the effect is easily obscured by changes in the friction factor.

For incompressible flow the area reduction as well as the sharp edge entrance causes a decrease in mass flow which is accounted for by contraction coefficients.[12,14]

Table 3 gives a summary of all the loss coefficients used in the computations.

Table 3. Loss and Flow Coefficients

$\alpha_e = 0.62$	$K_B = 5.04$
$\alpha_p = 0.64$	$K_F = 6.95$
$\alpha_g = 0.62$	$f = 0.0241$

Figure 6 shows a comparison between computed and experimental[2] pressure variations with time in the bolt cavity. It is seen that agreement between experiment and theory is quite satisfactory. The theoretical pressure is rising somewhat more slowly than the experimental value. This could be due to a friction coefficient somewhat too large in the early compressible phases of the flow. However, the fast experimental rise could more plausibly be explained by the fact that there is a component of dynamic pressure, resulting from the gas motion in the barrel itself, acting on the port, thus effectively increasing p_g; this would result in a larger influx in the bolt cavity, giving a correspondingly faster pressure rise. Indeed, this is suggested by the fact that barrel material is "washed out" downstream of the bore hole comprising the port. This same mechanism would also reduce the backward flow since the effective p_g is larger than indicated by the static pressure measurement. This is also borne out by the comparison. It is seen that the predicted pressure decreases faster than the experimental pressure; this is caused by too large a back flow. (See marker on Figure 6.) As has been pointed out above, the resistance due to deposits is also expected to be larger in the back flow than in the forward flow, and this has not been accounted for in the model.

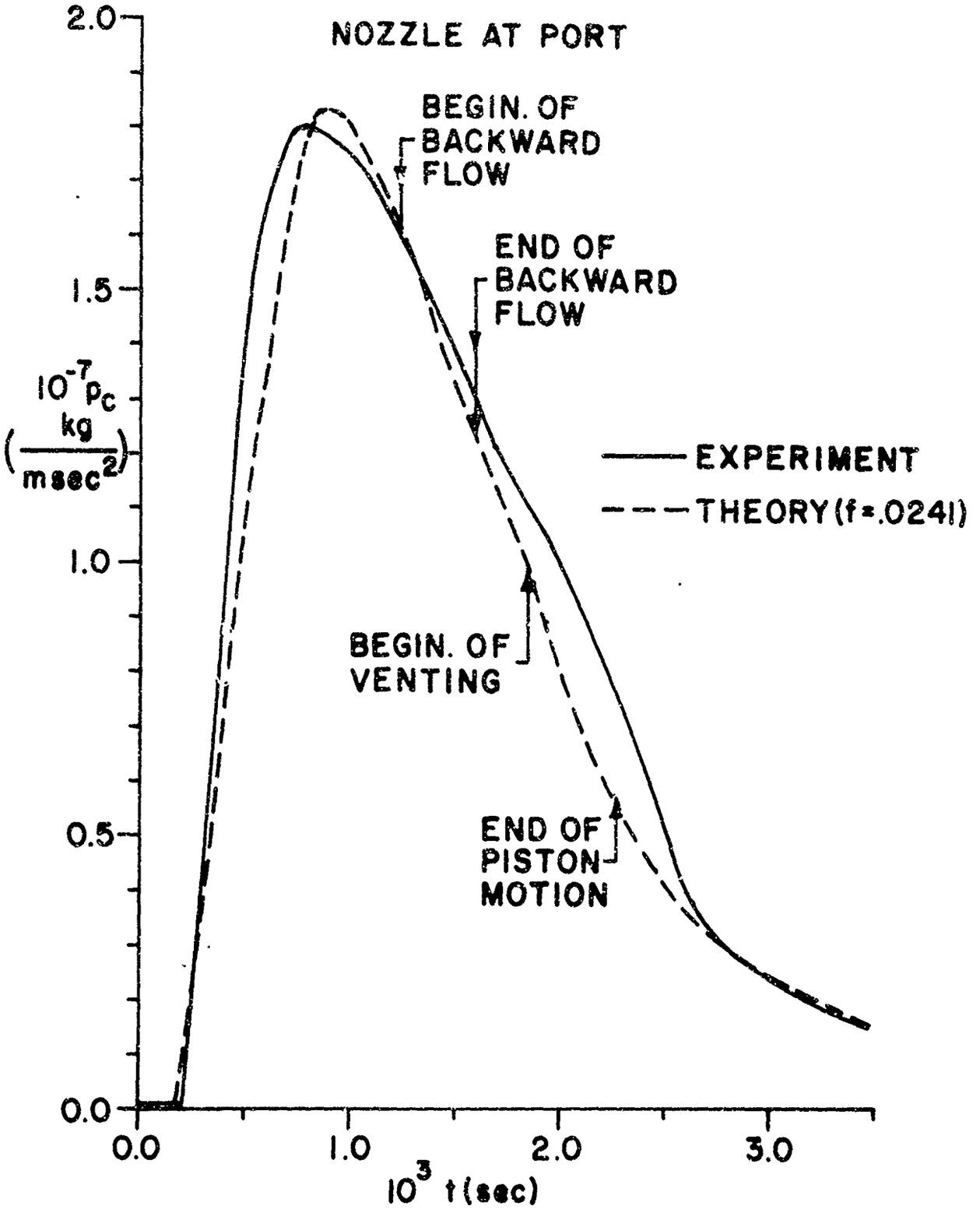

Figure 6. Comparison of Experimental and Theoretical Bolt Carrier Pressures for M-16 Rifle (Round 52)--Nozzle at Port

The measurements were made on a recoiling gun. This means that the piston displacement $\bar{x}_B$ is measured from an accelerated reference system. As a result there is an apparent force on the bolt carrier which opposes the bolt carrier motion. The measurement of gun motion indicates that the gun acceleration has dropped to nearly zero when the pressure starts to rise in the bolt cavity, so that only the early part of pressure history could be affected. It is worth noting that the net effect of the acceleration would result in a faster pressure rise than without the acceleration. The fast experimental pressure rise could indicate that the gun is still accelerating when the pressure starts rising in the cavity.

In this connection it should be mentioned that in the numerical computation the friction forces Φ on the bolt carrier were assumed zero. These are indeed expected to be small compared with the inertia force.

The venting area has been assumed to be the nominal area of the venting holes. Inspection of a number of guns indicates that this area may not be "cleared" completely by the bolt due to manufacturing tolerances. This would affect the tail of the pressure curve only and will not affect the motion of the bolt carrier.

Figure 7 shows the comparison of the experimental pressure trace with the computation where the area change is treated as a discontinuity. The computation based on the friction factor $f = 0.0241$ (same as in Figure 6) gives a somewhat lower pressure, but decreasing this friction factor by 25% gives essentially the same curve as shown on Figure 6. Since the friction factor is not believed to be known to better than 25%, it is not really possible to make a choice between the two models.

V. CONCLUSION

The analysis presented here gives the first term of an expansion in the parameter ε, which is the ratio of acoustical transit time to the characteristic time of pressure variation impressed on the flow in the actuation mechanism of the automatic weapons. Automatic weapons, by

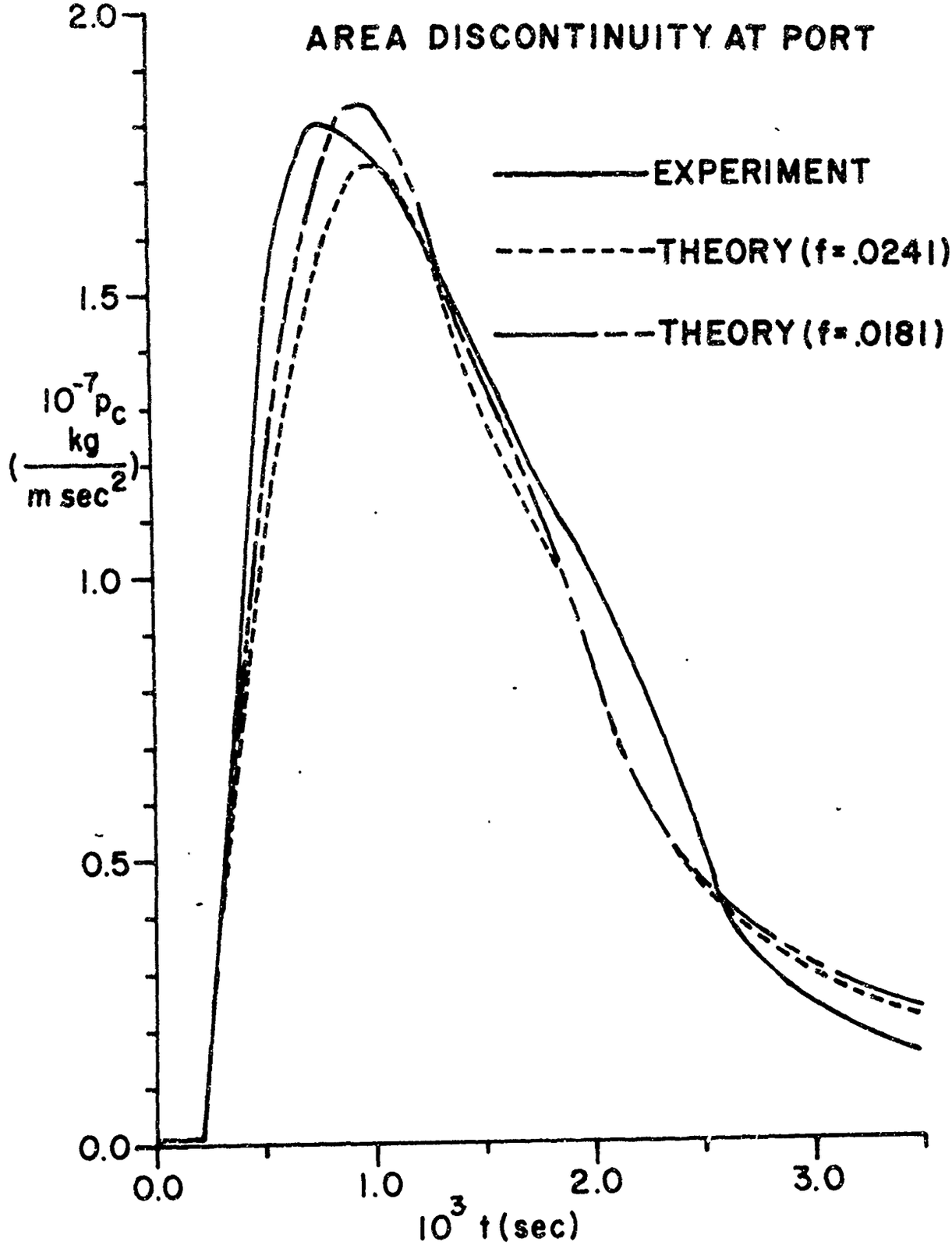

Figure 7. Comparison of Experimental and Theoretical Bolt Carrier Pressures for M-16 Rifle (Round 52)--Area Discontinuity at Port

necessity, are designed so that this parameter is small in order to assure quick responsive operation of the extracting and loading mechanism. Thus, although this analysis has only been tested for the M-16 rifle, it is expected to apply to other weapons and weapon systems also.

Most of the automatic weapons actually have considerably smaller values of ε because the length of the duct is very much shorter than it is the M-16 rifle and many weapons have no duct at all.[15] For these weapons the present analysis is also applicable, if the inner solution is completely discarded and the flow is treated as frictionless.

An approximate treatment for the M-16 rifle is obtained when the volume of the duct is added to initial volume and the inner solution is discarded. The heat losses due to heat transfer in the pipe have to be considered and may be accounted for globally in equation (3). This is the approach used in reference 2. In this treatment the initial condition is not fulfilled and the solution is not valid for small times; however, bolt velocity and bolt trajectory, which depend on integrals of the pressure distributions, are well predicted.

Most interesting would be the extension of this analysis to include second order terms. The characteristic time $\bar{\tau}$ does not appear explicitly in the first order solution; however, it should not be concluded that $\bar{\tau}$ is an "artificial" time. Actually, $\bar{\tau}$ will explicitly occur in the second approximation.

ACKNOWLEDGEMENT

It is a pleasure to thank Mr. N. Gerber for his very substantial help. He checked the various derivations and suggested many improvements, and he also conducted much of the numerical computations. The programming was done very competently by Miss B. Bilsborough. Thanks are due to Mr. H. Gay for suggesting this problem and to the personnel of Interior Ballistics Laboratory for providing the experimental results and for the help and encouragement they have given this project.

ADDENDUM

TREATMENT OF PORT AS AREA DISCONTINUITY

The assumption used in the body of the report treating the area constriction at the port as a frictionless supersonic nozzle is an artifice, especially since conditions are encountered which require a standing shock in the nozzle.

It may be more appropriate to treat the area constriction as an area discontinuity. In this case supersonic flow cannot be reached in the duct. Instead M_p is known from the integration of equation (24). Then the quantities at the throat (* quantities) may be computed from equations (36) and (37). Equation (36) is only applicable if $\overset{*}{p} < p_{crit}$; while for $\overset{*}{p} \geq p_{crit.}$ we have $\overset{*}{M} = 1$. It may be shown that the latter condition is equivalent to the condition

$$-\gamma + \sqrt{\frac{\gamma + 1}{2G}} \leq \omega$$

where G is given as $G(M_p)$ with equation (36). This inequality is always fulfilled for $M_p = 1$. Consideration of momentum

$$\overset{*}{p}\,\overset{*}{A}\,[1 + \gamma\,\overset{*}{M}^2] + p\,(A_p - \overset{*}{A}) = p_p\,A_p\,[1 + \gamma\,M_p^2]$$

then shows that $p \to 0$ for $\overset{*}{M} = M_p = 1$; i.e., the pressure on the surface $A_p - \overset{*}{A}$ is zero. (The control volume for application of the momentum equation is shown in Figure 8.)

The inner solution also has to be modified to account for the discontinuous area change. If the flow between throat and station p is considered steady, then $M_p = 1$ and the shock velocity follows from solving numerically

$$p_g(0)/p_i = \omega \left[\frac{2\hat{\gamma}}{\hat{\gamma}+1} M_s^2 - \frac{\hat{\gamma}-1}{\hat{\gamma}+1} \right] \left[\left(\frac{\gamma+1}{2} \right)^{1/2} - \frac{\gamma-1}{\hat{\gamma}+1} \frac{M_s^2-1}{M_s} \frac{a_i}{a_g(0)} \right]^{-\frac{2\gamma}{\gamma-1}}$$

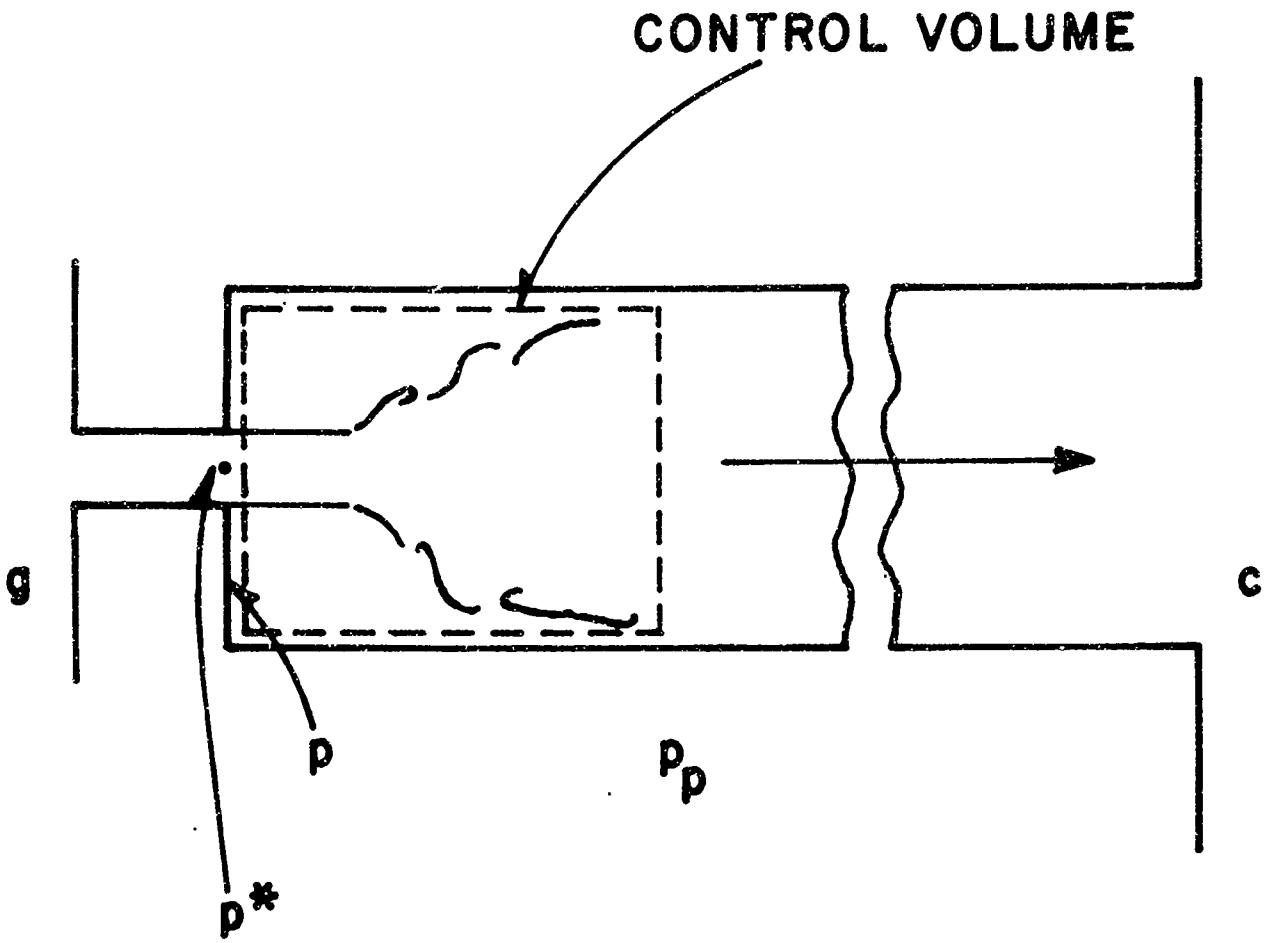

Figure 8. Sketch for Compressible Flow Treatment of Area Discontinuity at Port

The inner solution is shown in the X,T diagram of Figure 9. The relations (45), (47) and (48) are valid here also. The conditions at p now follow from (37) consistent with the assumption of steady flow between throat and station p. It is noted that the expansion fan now "reaches back" to station p and the inner solution affects the flow in the duct even for $T \to \infty$.

The condition $\overset{*}{M} = M_p = 1$ also makes the pressure on the area $A_p - \overset{*}{A}$ equal to zero, as has been noted before. It is worth pointing out that this steady flow condition is reached as the limit of the unsteady flow. The unsteady flow would result from the reflection of the expansion fan from the surface $A_p - \overset{*}{A}$; and for $\overset{*}{A} \ll A_p$ the reflection will be similar to the reflection of an expansion from a solid wall. It is well known that vacuum may result on the wall for a sufficiently large pressure ratio through the expansion fan.

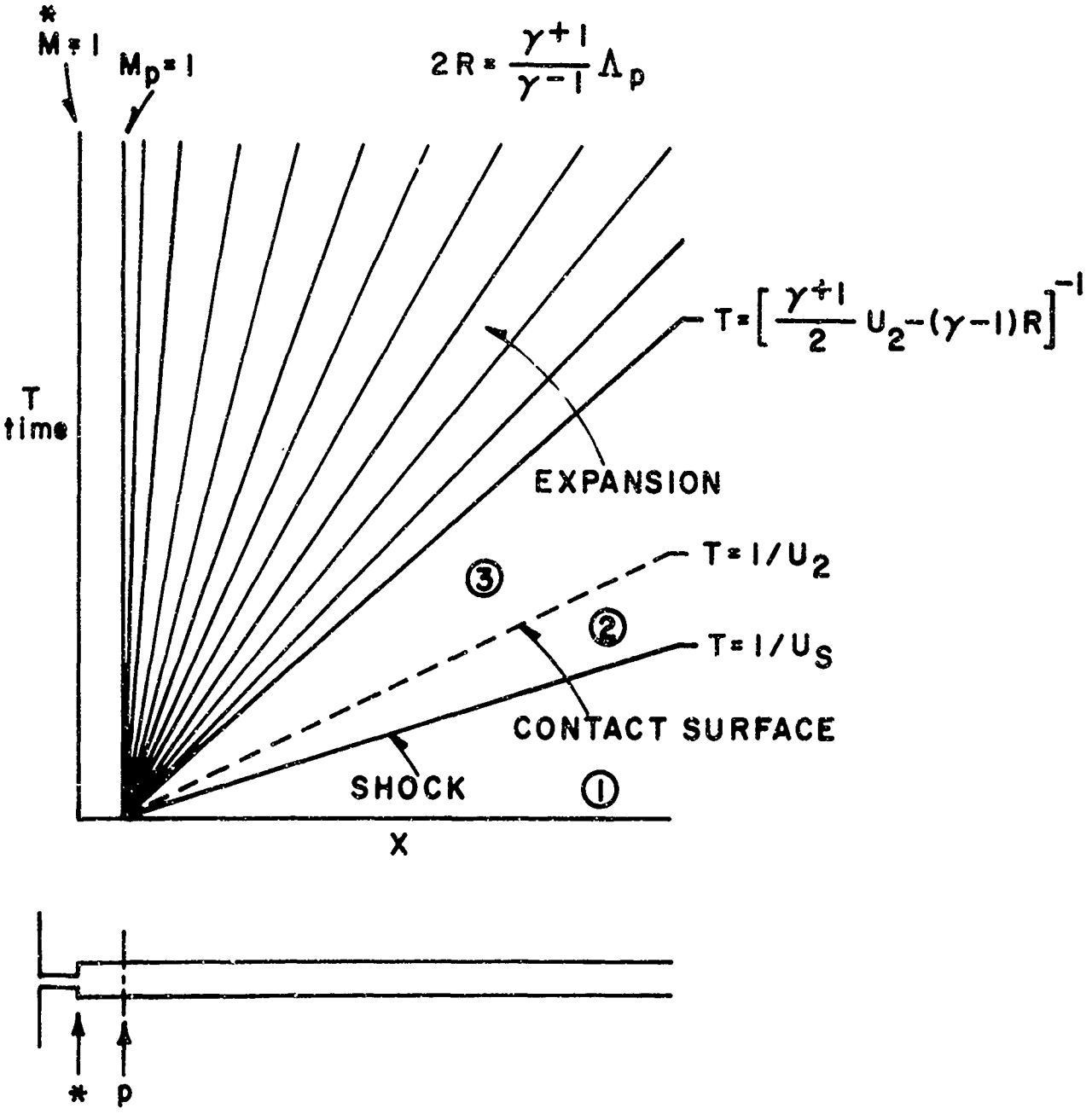

Figure 9. X, T Diagram for Inner Solution--Area Discontinuity at Port

REFERENCES

1. G. Rudinger, "Wave Diagrams for Nonsteady Flow in Ducts," D. Van Nostrand Co., New York, N.Y., 1955.

2. M. Werner, "Analysis of the Gas System of the M-16 Rifle," to be published as a Ballistic Research Laboratories Technical Note.

3. L. Crocco, Article in "High Speed Aerodynamics and Jet Propulsion," Vol. III (One-Dimensional Steady Gas Dynamics"), H. W. Emmons, Editor. Princeton University Press, Princeton, New Jersey, 1958.

4. A. H. Shapiro,"The Dynamics and Thermodynamics of Compressible Fluid Flow," Vol II., The Ronald Press Co., New York, N.Y., 1954.

5. E. Grashof, "Theoretische Maschinenlehre," Bd. 1, Leipzig, 1875.

6. A. H. Shapiro, "The Dynamics and Thermodynamics of Compressible Fluid Flow," Vol. I., The Ronald Press Co., New York, N.Y. 1953.

7. L. Prandtl, "Stromungslehre," F. Vieweg & Sohn, Braunschweig, 1956.

8. R. A. Alpher and D. R. White, "Flow in Shock Tubes with Area Change at the Diaphragm Section," Journal of Fluid Mech., Vol. 3, pp. 457-479, 1957-58.

9. J. H. Spurk, "Design, Operation, and Preliminary Results of the BRL Expansion Tube," Fourth Hypervelocity Techniques Symposium, Arnold Air Force Station, Tenn., 1965.

10. J. C. Camm and P. H. Rose, "Electric Arc-Driven Shock Tube," Physics of Fluids, Vol. 6, pp. 663-678, 1963.

11. M. Van Dyke, "Perturbation Methods in Fluid Dynamics," Academic Press, New York, N.Y., 1964.

12. Crane Technical Paper No. 410, "Flow of Fluids Through Valves, Fittings, and Pipe," Crane Co., Chicago, 1969.

13. C. L. Fulton, C. E. Shindler, and F. J. Shinaly, "Special Tests of 5.56MM Ammunition," Frankford Arsenal Report R-1883, February 1968.

14. E. V. Hütte, Des Ingenieurs Taschenbuch I (Theoretische Grundlagen), Wilhelm Ernst & Sohn, Berlin (1955).

15. W. H. B. Smith and J. E. Smith, Small Arms of the World, Stackpole Brothers, Harrisburg, Penna., Ninth Edition (1969).

APPENDIX A

DERIVATION OF EQUATION (36)

From the conservation of mass

$$\overset{*}{p}\,\overset{*}{A}\,\overset{*}{M} = p_p\, A_p\, M_p\, (\overset{*}{\theta}/\theta_p)^{1/2}$$

and momentum

$$\overset{*}{p}\,\overset{*}{A}\,(1 + \gamma\,\overset{*2}{M}) + \overset{*}{p}\,\overset{*}{A}\,(\omega-1) = p_p\, A_p\, (1 + \gamma\, M_p^{\,2})$$

there follows

$$(M_p/\overset{*}{M})\,(\overset{*}{\theta}/\theta_p)^{1/2}\,(\omega + \gamma\,\overset{*2}{M}) = 1 + \gamma\, M_p^{\,2}$$

Replacing $\overset{*}{\theta}/\theta_p$ by the energy equation (37) and solving a resulting quadratic equation for $\overset{*2}{M}$ lead to equation (36).

APPENDIX B

DERIVATION OF APPROXIMATE FLOW RELATIONS

The relation (38) for the flow velocity u at station e" (Figure 4), where the fluid again fills the total cross-sectional area of the duct, may be derived by first considering that the flow obeys Bernouilli's equation from station c to station e'. Thus

$$p_c - p_{e'} = \rho u_{e'}^2/2 \tag{B-1}$$

Between station e' and e" the spreading out of the jet occurs under losses, and application of conservation laws for mass and momentum leads to

$$p_{e'} - p_{e''} = \rho_e u_{e''}^2 [1 - (1/\alpha_e)] \tag{B-2}$$

where α_e is the contraction coefficient at station e. Combining (B-1) and (B-2) and applying conservation of mass gives:

$$p_c - p_{e''} = \frac{\rho_e u_{e''}^2}{2} \left[\left(\frac{1}{\alpha_e} - 1 \right)^2 + 1 \right] \tag{B-3}$$

Between stations e" and p integration of the momentum equation (21) yields

$$\rho_p u_p (u_p - u_{e''}) + p_p - p_{e''} + \frac{4 \rho_p^2 u_p^2 f}{2 \bar{D}} \int_0^{\bar{\ell}} \frac{1}{\rho} \, d\bar{x} = 0 \tag{B-4}$$

Combining (B-3) and (B-4), noting that $\rho_p = \rho_e = \rho_c = \text{const.}$, leads to

$$p_c - p_p = \frac{\rho_c u_{e''}^2}{2} \left[\left(\frac{1}{\alpha_e} - 1 \right)^2 + 1 + \frac{4 f \bar{\ell}}{\bar{D}} \right] \tag{B-5}$$

The pressure difference between stations p and g follows again by applying Bernouilli's equation between stations p and p' and the con-

servation laws between p' and g. Thus:

$$p_g - p_p = \frac{\rho_p u_p^2}{2} \left(1 - \omega^2 \left[1 + \left(\frac{1}{\alpha_p} - 1 \right)^2 \right] \right) \qquad \text{(B-6)}$$

Combining equations (B-5) and (B-6), noting that $u_p = u_e$ because $\rho_p = \rho_e$, gives equation (38).

Equation (41) can be derived in an analogous manner. First, the pressure difference between stations g and g" (Figure 4) is

$$p_g - p_{g"} = \frac{\rho_g u_{g"}^2}{2} \left[\left(\frac{1}{\alpha_g} - 1 \right)^2 + 1 \right] \qquad \text{(B-7)}$$

The pressure difference between stations g" and p is

$$p_{g"} - p_p = \omega^{-1} \rho_g u_{g"}^2 (\omega^{-1} - 1) \qquad \text{(B-8)}$$

so that the pressure difference between stations g and p is

$$p_g - p_p = \frac{\rho_g u_p^2}{2} \left[\left(\frac{\omega}{\alpha_g} - \omega \right)^2 + (\omega - 1)^2 + 1 \right] \qquad \text{(B-9)}$$

For the pressure difference between stations p and e

$$p_p - p_e = \rho_e u_e^2 [1 - (\rho_e/\rho_p)] + \frac{4 u_e^2 \rho_e^2 f}{2 \bar{D}} \int_0^{\bar{\ell}} \frac{1}{\rho} d\bar{x} \qquad \text{(B-10)}$$

From (B-9) and (B-10) one obtains equation (41), noting that for $p \neq fn(\rho)$

$$1/\rho = \theta_{tot}/(\rho_g \theta_g).$$

Unclassified

Security Classification

DOCUMENT CONTROL DATA - R & D

(Security classification of title, body of abstract and indexing annotation must be entered when the overall report is classified)

1. ORIGINATING ACTIVITY (Corporate author) Aberdeen Research and Development Center USA Ballistic Research Laboratories Aberdeen Proving Ground, Maryland 21005	2a. REPORT SECURITY CLASSIFICATION Unclassified 2b. GROUP

3. REPORT TITLE

THE GAS FLOW IN GAS-OPERATED WEAPONS

4. DESCRIPTIVE NOTES (Type of report and inclusive dates)

5. AUTHOR(S) (First name, middle initial, last name)

Joseph H. Spurk

6. REPORT DATE	7a. TOTAL NO. OF PAGES	7b. NO. OF REFS
February 1970	68	15

8a. CONTRACT OR GRANT NO. b. PROJECT NO. 1T061102A33D c. d.	9a. ORIGINATOR'S REPORT NUMBER(S) BRL Report No. 1475 9b. OTHER REPORT NO(S) (Any other numbers that may be assigned this report)

10. DISTRIBUTION STATEMENT

This document has been approved for public release and sale; its distribution is unlimited.

11. SUPPLEMENTARY NOTES	12. SPONSORING MILITARY ACTIVITY
None	U. S. Army Materiel Command Washington, D. C.

13. ABSTRACT

In gas-operated weapons, the time-varying pressure in the barrel is fed through a duct into a cylinder. The piston in the cylinder is displaced by the pressure and operates on a mechanism which extracts the spent cartridge and completes the next loading cycle.

The theory presented here predicts the pressure history in the cylinder and the motion of the piston for a given pressure and temperature history in the barrel.

DD FORM 1 NOV 65 1473 REPLACES DD FORM 1473, 1 JAN 64, WHICH IS OBSOLETE FOR ARMY USE.

Unclassified

Security Classification

Unclassified
Security Classification

14. KEY WORDS	LINK A		LINK B		LINK C	
	ROLE	WT	ROLE	WT	ROLE	WT
Automatic Weapons						
Compressible Unsteady Heat-Conducting Flow						
Gasdynamics						
Rifle						
Singular Perturbations						
Unsteady Flow						

Unclassified
Security Classification